國立交通大學

應用數學系

碩 士 論 文

求解離子通道之

二階 Poisson Nernst-Planck 簡化法

A simplified second-order Poisson Nernst-Planck solver for ion channel

研　究　生: 楊祥鶴

指 導 教 授：劉晉良　博士

共同指導教授：吳金典　博士

中 華 民 國 一 百 零 一 年 六 月

求解離子通道之二階 Poisson Nernst-Planck 簡化法

A simplified second-order Poisson Nernst-Planck solver for ion channel

研 究 生：楊祥鶴　　Student : Shiang-He Yang

指 導 教 授：劉晉良　博士　　Advisor : Jinn-Liang Liu

共同指導教授：吳金典　博士　　Co-advisor : Chin-Tien Wu

國立交通大學

應用數學系

碩 士 論 文

A Thesis

Submitted to Department of Applied Mathematics

College of Science

National Chiao Tung University

in Partial Fulfillment of the Requirements

for the Degree of

Master

In

Applied Mathematices

June 2012

Hsinchu, Taiwan, Republic of China

中 華 民 國 一 百 零 一 年 六 月

求解離子通道之二階 Poisson Nernst-Planck 簡化法

學生:楊祥鶴　　指 導 教 授：劉晉良

共同指導教授：吳金典

國立交通大學應用數學系（研究所）碩士班

摘要

本論文運用基本的 Poisson Nernst-Planck(PNP)數學模型來模擬生物細胞的離子通道在穩定狀態的情形,然而 Poisson 方程式可經由庫倫定律和高斯定理來獲得,至於 Nernst-Planck 方程式則是等價於漂移擴散數學模型,過去很多的計算方法都已經被應用在 PNP 數學模型上,然而我們的主要目的是去簡化在[24]裡面的計算方法,並且保持二階收斂的效果,但我們有一些必須要去處理的問題,例如我們應用位能分解方法[5]去處理 Delta 函數,使用合適的介面和邊界(matched interface and boundary)方法 [24]來處理不同介質的問題,而對於初始值猜測則必須由 Poisson Boltzmman 方程得到,最後我們由分子資料銀行(protein data bank)得到真實的短杆菌肽(Gramicidin A)通道的資訊並且建構它的幾何結構。

A simplified second-order Poisson Nernst-Planck solver for ion channel

Student: Shiang-He Yang[1] Advisor: Jinn-Liang Liu[2], Chin-Tien Wu[1]
[1]Department of Applied Mathematics
National Chiao Tung University
[2]Department of Applied Mathematics
National Hsinchu University of Education

July 3, 2012

Abstract

The Poisson-Nernst-Planck (PNP) model is a basic continuum model for simulating ionic flows in an open ion channel. It is one of commonly used models in theoretical and computational. The Poisson equation is derived from Coulomb's law in electrostatics and Gauss's theorem in calculus. The Nernst-Planck equation is equivalent to the convection-diffussion model. Many computation methods have been constructed for the solution of the PNP equations. However, we want to simplify the second order solver of proposed in the literature [24] but, we must to deal with some problems. For example, singular charges, nonlinear coupling and interface. First, we apply the decomposition method [5] proposed by Chern, Liu and Wang to cope with the singular charges. Second, the matched interface and boundary (MIB) method [24] is used for the interface problem. Third, the initial guess are given by Poisson Boltzmann (PB) equation and two iterative schemes are utilized to deal with the coupled nonlinear equations. Finally, the real data of Gramicidin A (GA) channel protein is obtained from the protein data bank (PDB).

誌謝

本篇論文的完成,首先感謝我的指導老師劉晉良博士,在這二年間的悉心教誨,而劉老師雄厚的物理知識以及在半導體上的豐富經驗,也幫助我運用在生物系統上解決了很多的問題,在此獻上我最誠摯的感謝。另外也感謝我的共同指導老師吳金典博士,老師所教授的有限元素方法用途非常的廣而理論架構也相當完整,我相信對我的未來發展一定有相當大的幫助。

同時感謝我的口試委員陳人豪教授和彭振昌教授,於口試期間的建議以及對疏漏處的提醒和指正。

而在交大應數的這兩年,無論是在課堂上,亦或是參與各種演講和研討會,都讓我學習到做研究的精神與態度,在此感謝所有我修過課的老師們以及我所參加過的演講的所有教授們。再來我要感謝所有在碩班認識的同學、學長姐和學弟妹。以及在系壘認識的各位,在我的研究生生涯中,因爲有你們的陪伴,我的生活才得以充實,充滿歡笑與快樂,謝謝你們。

在這邊,我要特別感謝我的家人以及女友,一直在背後支持、陪伴和鼓勵著我,謝謝爸爸和媽媽提供給我很好的環境和資源,讓我在我的學生生涯能夠無後顧之憂,在我的求學的路上也沒有給我任何壓力,並尊重我做的任何決定。能夠順利完成這篇論文,這份榮耀我要與你們分享,也希望我能成爲你們的驕傲。

楊祥鶴

謹誌于交通大學

2012 年六月

Contents

1 Introduction

Biological ion channel is a porous protein on cell membrane and they are present in the membranes that surround all biological cells. It allows some particular ions across cell membrane and then controls the electrical potential difference of the internal and exterior part. These ions move through the channel pore single file nearly as quickly as the ions move through free fluid. In some ion channels, passage through the pore is governed by a "gate" which may be opened or closed by chemical or electrical signals, temperature, or mechanical force..., depending on the variety of channel. Ion channel is vary important for process of life such as control hormone ooze, preservation of salt and water balance, sensory transduction, nerve and muscle excitation, muscle contraction etc. [13], in general, ion channels may be classified by the nature of their gating, species of ions passing through those gates or the number of gates (pores) and localization of proteins. Moreover, ion channels may be classified by gating, i.e., what opens and closes the channels. For example, voltage-gated ion channels open or close depending on the voltage gradient across the plasma membrane, while ligand-gated ion channels open or close depending on binding of ligands to the channel.

The following is some of the most important development of ion channels, British biophysicists Alan Hodgkin and Andrew Huxley discoveries concerning "the ionic mechanisms in the nerve cell membrain" (Nobel Prize in Physiology or Medicine 1963), Erwin Neher and Bert Sakmann discoveries concerning "the function of single ion channels in cells" (Nobel Prize in Physiology or Medicine 1991). Roderick MacKinnon for his studies on the physico-chemical properties of ion channel structure and function, including x-ray crystallographic structure studies, and Peter Agre for his similar work on aquaporins (Nobel Prize in Chemistry 2003). In the past decades many experimental techniques have been well-developed for study ion channels [14]. However, this data has driven the development of the theory and calculations. The commonly used method are ab initio molecular dynamics (MD) and classical molecular dynamics (MD) [19]. Because taking into account each ion, it requires a very large number of computing.

The Poisson-Nernst-Planck (PNP) equations are an approximation of ions, for which we do not deal with a discrete distribution for the ions. Instead, we consider continuous charge densities. The PNP theory considers the real channel structure and discrete protein charge locations in its modeling and computation. The PNP theory neglects the finite volume effect of ion particles, which can be important for small channel pores [16]. The existence and uniqueness of PNP equation is an important issue in mathematics and on certain restrictions can be obtained [2][3][10]. Due to the overly complex domain, analytic solution to the original PNP system is unfeasible. Therefore, we focus on the numerical solution and thus understand the meaning of the results. PNP is a very interesting

model that includes three coupled equations, irregular geometry, discontinuous dielectric coefficients, singular charges and nonlinearity.

In mathematics, a lot of discrete methods have been used to solve the PNP equation, such as finite diifference method, finite element method, finite volume method and spectral element method. Among them Q. Zheng, D. Chen and G. W. Wei provide a second-order convergeence method [24] and this is first method that yields a second-order convergence in the literature for three-dimensional (3D) realistic geometry of the Gramicidin A(GA) channel, but the method requires up to 27 finite difference points. We simplify this difference method to seven points formula and maintain the quadratic convergence. For initial guess, the potential is obtained by Poisson-Boltzmann (PB) [23] equation and it is a nonlinear equation. The PB equation will be solved by linearized PB equation as initial guess and then will need to implement monotone iterative method [17] to solve nonlinear PB equation. For the singular charge, we implemant the decomposition method proposed by Chern, Liu, and Wang [5] and the potential is decomposed into three parts such that delta function disappears in the right hand side. Because we use this decomposition method [5], we must approximate the gradient of the Green function (section 2.2.4 and 4.3). For interface problem, the match interface and boundary (MIB) method is used to connect solvent and molcular parts and to treat jump conditions.

For channel structure, Visual Molecular Dynamics (VMD) [15] is designed for modeling, visualization, and analysis of biological systems such as proteins, nucleic acids, lipid bilayer assemblies, etc. It may be used to view more general molecules, as VMD can read standard Protein Data Bank (PDB) files and display the contained structure. VMD can be used to animate and analyze the trajectory of a molecular dynamics (MD) simulation. In particular, VMD can act as a graphical front end for an external MD program by displaying and animating a molecule undergoing simulation on a remote computer. We consider water in the channel and generate Molecular Surface (interface) in 3D uniform grid by van der Waas radii and a probe ball, i.e., closest distance of water molecules with protein that is obtained by VMD.

2 Poisson-Nernst-Planck model and numerical methods

Biological ion channels seem to be a precondition for all living matter [20]. Ion channels are porous proteins across cell membranes that control many biological functions ranging from signal transfer in the nervous system to regulation of secretion of hormones. Understanding the mechanism of ionic flows within a channel as a function of ionic concentration, membrane potential, and the structure of the channel is a central problem in

molecular biophysics [12]. The PNP model proposed by Eisenberg and coworkers [8][9] as a basic continuum model for simulating the ionic flow in an open ion channel is one of commonly used models in theoretical and computational studies of biological ion channels.

2.1 Poisson-Nernst-Planck model

For modeling the flow of two species of ions through a channel, the steady-state PNP model (2.1.1)-(2.1.3) reads as [24]

$$\begin{aligned}
\text{P} \quad &: \quad -\nabla \cdot (\epsilon(r)\nabla\phi(r)) = 4\pi \sum_{j=1}^{N_A} q_j \delta(r - r_j) + 4\pi \sum_{i=1}^{2} q_i C_i(r), \ r \in \Omega \qquad (2.1.1)\\
\text{NP1} \quad &: \quad -\nabla \cdot J_1(r) = 0, \ r \in \Omega_s \qquad (2.1.2)\\
\text{NP2} \quad &: \quad -\nabla \cdot J_2(r) = 0, \ r \in \Omega_s \qquad (2.1.3)\\
J_i(r) \quad &= \quad -D_i(r)\left[\nabla C_i(r) + \beta_i C_i(r)\nabla\phi(r)\right] \text{ for i = 1, 2} \qquad (2.1.4)\\
\phi^*(r) \quad &= \quad 4\pi \sum_{j=1}^{N_A} q_j \delta(r - r_j) \approx \sum_{j=1}^{N_A} \frac{q_j}{\epsilon_m \sqrt{(x-x_j)^2 + (y-y_j)^2 + (z-z_j)^2}} \qquad (2.1.5)
\end{aligned}$$

where $r = (x, y, z)$, $J_i(r)$ is the current density of an ion species i with q_i, $C_i(r)$ is the concentration of an ion species i carrying charge q_i (for example,$q_{k^+} = +1e, q_{cl^-} = -1e$), J_i the concentration flux (current density), D_i the spatially dependent diffusion coefficient, $\beta_i = q_i/(k_B T)$, k_B the Boltzmann constant, T the absolute temperature, ϕ the electrostatic potential, ϵ the dielectric constant , and e the protein charge. The domain $\overline{\Omega} = \overline{\Omega}_m \cup \overline{\Omega}_s$ consists of two subdomains, namely, the solvent subdomain $\overline{\Omega}_s$ and the biomolecular subdomain$\overline{\Omega}_m$. The electric permittivity has different values in subdomains and denoted by

$$\epsilon(r) = \epsilon_r = \begin{Bmatrix} \epsilon_s, \forall r \in \Omega_s \\ \epsilon_m, \forall r \in \Omega_m \end{Bmatrix} \qquad (2.1.6)$$

where $\epsilon_r = \epsilon_s$ is the dielectric constant of the solvent, and $\epsilon_r = \epsilon_m$ is the dielectric constant of the molecules. We consider the domain as a cubical box

$$\text{Box} = \Omega = (-20\mathring{A}, 20\mathring{A}) \times (-20\mathring{A}, 20\mathring{A}) \times (0\mathring{A}, 40\mathring{A}) \qquad (2.1.7)$$

For the jump condition at the interface Γ given by

Poisson equation:

$$[\phi(r)] = \phi^+ - \phi^- = 0,\ r \in \Gamma \tag{2.1.8}$$

$$[\epsilon(r)\phi_n(r)] = \epsilon_m \nabla\phi^+ \cdot n - \epsilon_s \nabla\phi^- \cdot n = 0,\ r \in \Gamma \tag{2.1.9}$$

Nernst-Planck:

$$J_i(r) \cdot n = 0,\ r \in \Gamma \tag{2.1.10}$$

where

$$\Gamma = \overline{\Omega}_m \cap \overline{\Omega}_s \tag{2.1.11}$$

$$\phi^+ = \lim_{x \to r^+} \phi(x),\ \phi^- = \lim_{x \to r^-} \phi(x),\ r^- \in \Omega_s,\ r^+ \in \Omega_m \tag{2.1.12}$$

Γ is the interface set between Ω_s and Ω_m, n is an outward normal unit vector on Γ and $\mathring{A}$ is equal to $10^{-8} cm(Length)$.

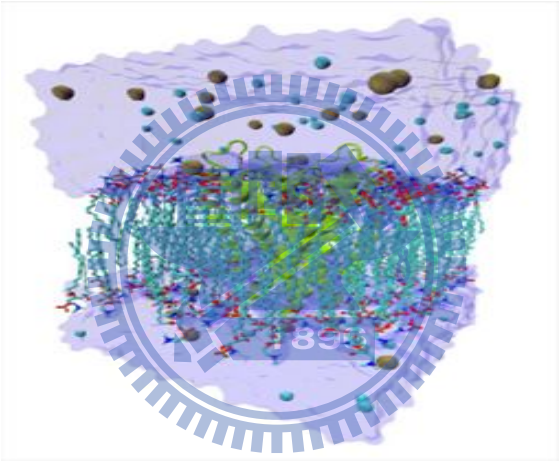

Figure 1: VMD simulation system of the KcsA channel with membrane, water,and ions.

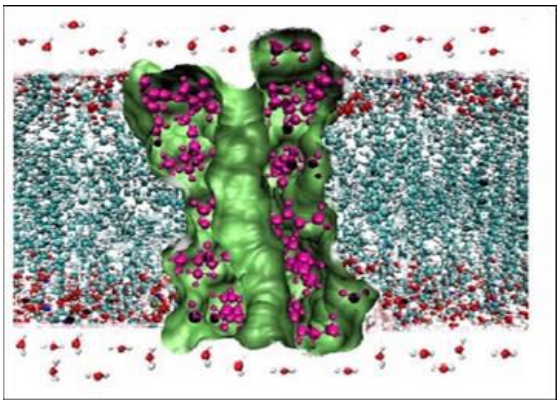

Figure 2: Side view of the GA channel embedded in the membrane.

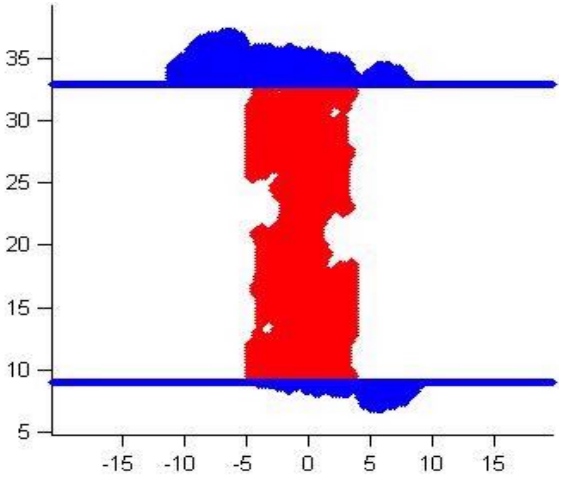

Figure 3: Constructed domain

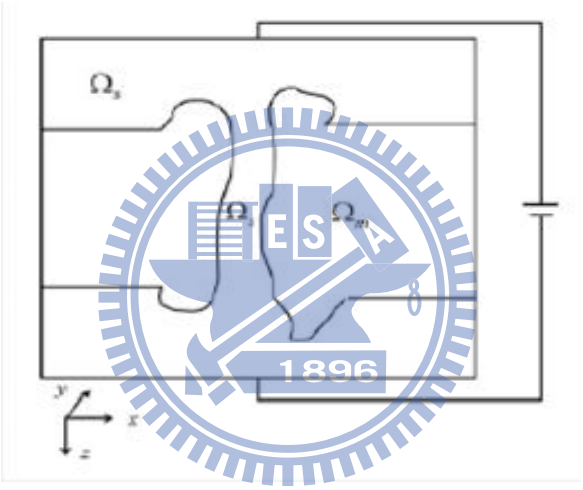

Figure 4: A cross section of 3D PNP simulation domain for GA channel.

Fig. 4 is across section of 3D PNP simulation domain for the GA channel [7]. Fig. 2 is a side view of the GA channel embedded in the membrane [24]. Fig. 1 illustrates a VMD [15] simulation system of the KcsA channel with membrane, water, and ions [1]. The channel protein is in the central part of the simulation domain (a box) as shown in green color. The membrane consists of bilipid layers shown in light blue surrounding the channel. The upper and lower regions represent the extracellular (outside of a cell) and intracellular (inside) solvent regions, respectively, that consist of water and ions.

2.2 Numerical methods for PNP

2.2.1 Finite difference method for Poisson's equation

Discretization of the left hand side of (2.1.1) by the central finite difference method (FDM) yields

$$-\frac{\partial}{\partial x}(\epsilon(r)\frac{\partial\phi(x_i,y,z)}{\partial x}) \approx \frac{-\epsilon_{i-\frac{1}{2}}\phi_{i-1}+(\epsilon_{i-\frac{1}{2}}+\epsilon_{i+\frac{1}{2}})\phi_i-\epsilon_{i+\frac{1}{2}}\phi_{i+1}}{\Delta x^2} \tag{2.2.1}$$

for all $(x_i,y,z)\in\Omega_m\cup\Omega_s$, $\frac{\partial\phi(x,y,z)}{\partial x}=\phi_x$, $\phi_i=\phi(x_i,y,z)$, $\Delta x=x_i-x_{i-1}=h$, and x_i are finite difference grid points. We assume a uniform partition of the box in each direction, i.e., $\Delta x=\Delta y=\Delta z=h$. To simplify the notation, we write (2.1.1) in 1D as

$$-\frac{\partial}{\partial x}(\epsilon(x)\frac{\partial\phi(x)}{\partial x})=f \tag{2.2.2}$$

The second-order, denoted by O(h^2) (convergence order is 2), central FD approximation of (2.2.2) is

$$\frac{-\epsilon_{i-\frac{1}{2}}\phi_{i-1}+(\epsilon_{i-\frac{1}{2}}+\epsilon_{i+\frac{1}{2}})\phi_i-\epsilon_{i+\frac{1}{2}}\phi_{i+1}}{\Delta x^2}=f_i \tag{2.2.3}$$

For interface problem, we alway assume that

$$x_{i-1}<\gamma=x_{i-\frac{1}{2}}<x_i \tag{2.2.4}$$

i.e., every jump position $\gamma\in\Gamma$ is at the middle of some neighboring grid points. We consider the following jump condition for Poisson problem (2.1.8) (2.1.9)

$$[\phi(r)] = \phi^+-\phi^-=0,\ r\in\Gamma \tag{2.2.5}$$

$$[\epsilon(r)\phi_n(r)] = \epsilon_m\nabla\phi^+\cdot n-\epsilon_s\nabla\phi^-\cdot n=0,\ r\in\Gamma \tag{2.2.6}$$

For the jump condition in 1D, we have

$$[\epsilon(r)\phi_n(r)]=\epsilon_m\nabla\phi^+\cdot n-\epsilon_s\nabla\phi^-\cdot n=\epsilon_m\phi_x^+-\epsilon_s\phi_x^-,\ n=(1,0,0) \tag{2.2.7}$$

or

$$[\epsilon(r)\phi_n(r)]=\epsilon_m\nabla\phi^+\cdot n-\epsilon_s\nabla\phi^-\cdot n=-\epsilon_m\phi_x^++\epsilon_s\phi_x^-,\ n=(-1,0,0) \tag{2.2.8}$$

Remark. 2. 1: By (2.1.8) and (2.1.9), it is easy to observe that the electrostatic potential ϕ is continuous and non-differential on Γ.

2.2.2 Matched interface and boubdary method (MIB)

For different dielectric constant ϵ_m, ϵ_s and the non-differential point, the MIB is used to deal with this problem such that we can obtain a second-order convergence formula. The main ideas of the MIB method for handling the jump problem are

(1) considering (2.2.2) as two different subproblems with two disjoint subdomain $x < \gamma$ and $x > \gamma$,

(2) taking the jump condition (2.2.5) and (2.2.6) as the boundary conditions for each subproblem with respect to its subdomain,

(3) extending smoothly a function $\phi(x)$ defined on a subdomain to a 'fictitious' function $\Psi(x)$ defined on another subdomain, and

(4) applying Taylor's theorem to the jump conditions for joining two subproblems back to one.

Define the extension functions

$$F(x) = \begin{cases} \phi(x) \text{ , if } x<\gamma \\ \Psi(x), \text{ if } x\geq\gamma \end{cases} \text{ or } G(x) = \begin{cases} \phi(x) \text{ , if } x>\gamma \\ \Psi(x), \text{ if } x\leq\gamma \end{cases} \tag{2.2.9}$$

Applying Taylor's theorem to $F(x)$ at the interface, we have

$$F(x_{i-1}) = F(\gamma) + F'(\gamma)(x_{i-1}-\gamma) + \frac{F'(\gamma)}{2!}(x_{i-1}-\gamma)^2 + O(h^3) \tag{2.2.10}$$

$$F(x_i) = F(\gamma) + F'(\gamma)(x_i-\gamma) + \frac{F'(\gamma)}{2!}(x_i-\gamma)^2 + O(h^3) \tag{2.2.11}$$

$$F(\gamma) = \frac{F(x_{i-1}) + F(x_i)}{2} + O(h^2) \tag{2.2.12}$$

Hence, for (2.2.5) we have

$$\phi^- = F(\gamma) = \frac{\phi_{i-1} + \Psi_i}{2} + O(h^2) \tag{2.2.13}$$

$$\phi^+ = G(\gamma) = \frac{\phi_i + \Psi_{i-1}}{2} + O(h^2) \tag{2.2.14}$$

$$[\phi] = \frac{\phi_i + \Psi_{i-1}}{2} - \frac{\phi_{i-1} + \Psi_i}{2} + O(h^2) \tag{2.2.15}$$

Similarly for (2.2.6), subtracting (2.2.10) from (2.2.11) gives

$$hF'(\gamma) = F(x_i) - F(x_{i-1}) + O(h^3) \tag{2.2.16}$$

$$\phi_x^- = F'(\gamma) = \frac{\Psi_i - \phi_{i-1}}{h} + O(h^2) \tag{2.2.17}$$

$$\phi_x^+ = G'(\gamma) = \frac{\phi_i - \Psi_{i-1}}{h} + O(h^2) \tag{2.2.18}$$

$$[\epsilon\phi_x] = \epsilon_m \frac{\phi_i - \Psi_{i-1}}{h} - \epsilon_s \frac{\Psi_i - \phi_{i-1}}{h} + O(h^2) \tag{2.2.19}$$

Therefore, by (2.2.15) and (2.2.19), the following equations

$$A_1\phi_{i-1} + A_2\Psi_i = A_3\Psi_{i-1} + A_4\phi_i - [\phi] \tag{2.2.20}$$

$$\epsilon^-(B_1\phi_{i-1} + B_2\Psi_i) = \epsilon^+(B_3\Psi_{i-1} + B_4\phi_i) - [\epsilon\phi_x] \tag{2.2.21}$$

represent FD approximations of (2.2.5) and (2.2.6), respectively, with local truncation errors of $O(h^2)$. Here, the weight are

$$A_1 = A_2 = A_3 = A_4 = \frac{1}{2} \tag{2.2.22}$$

$$B_1 = B_3 = \frac{-1}{h}, B_2 = B_4 = \frac{-1}{h} \tag{2.2.23}$$

Solving (2.2.20) and (2.2.21) for the fictitious values Ψ_i and Ψ_{i+1} we obtain

$$\begin{aligned}\Psi_{i-1} &= \frac{(\epsilon^- B_2A_1 - \epsilon^+ B_1A_2)\phi_{i-1} - (\epsilon^- B_2A_4 - \epsilon^+ B_4A_2)\phi_i}{\epsilon^- B_2A_3 - \epsilon^+ B_3A_2} \\ &\quad + \frac{\epsilon^- B_2[\phi] - A_2[\epsilon\phi_x]}{\epsilon^- B_2A_3 - \epsilon^+ B_3A_2} \\ &= C_1\phi_{i-1} + C_2\phi_i + C_0 \end{aligned} \tag{2.2.24}$$

$$\begin{aligned}\Psi_i &= \frac{-(\epsilon^+ B_3A_1 - \epsilon^- B_1A_3)\phi_{i-1} + (\epsilon^+ B_3A_4 - \epsilon^+ B_4A_2)\phi_i}{\epsilon^+ B_3A_2 - \epsilon^- B_2A_3} \\ &\quad + \frac{-\epsilon^+ B_3[\phi] + A_3[\epsilon\phi_x]}{\epsilon^+ B_3A_2 - \epsilon^- B_2A_3} \\ &= D_1\phi_{i-1} + D_2\phi_i + D_0 \end{aligned} \tag{2.2.25}$$

Following (2.2.3) by differencing $F(x)$ at the grid point x_{i-1} and differencing $G(x)$ at the grid point x_i , we obtain

$$\frac{-\epsilon_{i-\frac{3}{2}}\phi_{i-2} + (\epsilon_{i-\frac{3}{2}} + \epsilon^-_{i-\frac{1}{2}})\phi_{i-1} - \epsilon^-_{i-\frac{1}{2}}\Psi_{i+1}}{\Delta x^2} = f_{i-1} \tag{2.2.26}$$

$$\frac{-\epsilon^+_{i-\frac{1}{2}}\Psi_{i-1} + (\epsilon^+_{i-\frac{1}{2}} + \epsilon_{i+\frac{1}{2}})\phi_i - \epsilon_{i+\frac{1}{2}}\phi_{i+1}}{\Delta x^2} = f_i \tag{2.2.27}$$

Although Ψ_i and Ψ_{i-1} are called ficitious (ghost) value, they are real in implemantation and defined by (2.2.24) (2.2.25) via ϕ_{i-1} and ϕ_i. Consequently, (2.2.26) and (2.2.27) become

$$\frac{-\epsilon_{i-\frac{3}{2}}\phi_{i-2}+(\epsilon_{i-\frac{3}{2}}+(1-D_1)\epsilon^-_{i-\frac{1}{2}})\phi_{i-1}-D_2\epsilon^-_{i-\frac{1}{2}}\phi_i}{\Delta x^2} = f_{i-1}+\frac{\epsilon^-_{i-\frac{1}{2}}D_0}{\Delta x^2} \quad (2.2.28)$$

$$\frac{-C_1\epsilon^+_{i-\frac{1}{2}}\phi_{i-1}+((1-C_2)\epsilon^+_{i-\frac{1}{2}}+\epsilon_{i+\frac{1}{2}})\phi_i-\epsilon_{i+\frac{1}{2}}\phi_{i+1}}{\Delta x^2} = f_i+\frac{\epsilon^+_{i-\frac{1}{2}}C_0}{\Delta x^2} \quad (2.2.29)$$

or (by $\gamma = x_{i-\frac{1}{2}}$)

$$\frac{-\epsilon_s\phi_{i-2}+(\epsilon_s+(1-D_1)\epsilon_s)\phi_{i-1}-D_2\epsilon_s\phi_i}{\Delta x^2} = f_{i-1}+\frac{\epsilon_s D_0}{\Delta x^2} \quad (2.2.30)$$

$$\frac{-C_1\epsilon_m\phi_{i-1}+((1-C_2)\epsilon_m+\epsilon_m)\phi_i-\epsilon_m\phi_{i+1}}{\Delta x^2} = f_i+\frac{\epsilon_m C_0}{\Delta x^2} \quad (2.2.31)$$

$$\begin{aligned}&\frac{-C_1\epsilon_m\phi_{i-1,j}+((1-C_2)\epsilon_m+\epsilon_m)\phi_{i,j}-\epsilon_m\phi_{i+1,j}}{\Delta x^2}\\ &+\frac{-C_1\epsilon_m\phi_{i,j-1}+((1-C_2)\epsilon_m+\epsilon_m)\phi_{i,j}-\epsilon_m\phi_{i,j+1}}{\Delta x^2}\\ &= f_{ij}+\frac{\epsilon_m C_0}{\Delta x^2}+\frac{\epsilon_s D_0}{\Delta x^2}, \text{(for 2 jumps in 2D)}\end{aligned} \quad (2.2.32)$$

whewe

$$C_1 = \frac{(\epsilon^- B_2A_1-\epsilon^+B_1A_2)}{\epsilon^-B_2A_3-\epsilon^+B_3A_2}=\frac{\epsilon_sB_2-\epsilon_sB_1}{\epsilon_sB_2-\epsilon_mB_3}=\frac{2\epsilon_s}{\epsilon_s+\epsilon_m} \quad (2.2.33)$$

$$C_2 = \frac{-(\epsilon^- B_2A_4-\epsilon^+B_4A_2)}{\epsilon^-B_2A_3-\epsilon^+B_3A_2}=\frac{-\epsilon_sB_2+\epsilon_mB_4}{\epsilon_sB_2-\epsilon_mB_3}=\frac{\epsilon_m-\epsilon_s}{\epsilon_s+\epsilon_m} \quad (2.2.34)$$

$$C_0 = \frac{\epsilon^- B_2[\phi]-A_2[\epsilon\phi_x]}{\epsilon^-B_2A_3-\epsilon^+B_3A_2}=\frac{2\epsilon_sB_2[\phi]-[\epsilon\phi_x]}{\epsilon_sB_2-\epsilon_mB_3}=\frac{2\epsilon_s[\phi]-h[\epsilon\phi_x]}{\epsilon_s+\epsilon_m} \quad (2.2.35)$$

$$D_1 = \frac{-(\epsilon^+ B_3A_1-\epsilon^-B_1A_3)}{\epsilon^+B_3A_2-\epsilon^-B_2A_3}=\frac{-(\epsilon_mB_3-\epsilon_sB_1)}{\epsilon_mB_3-\epsilon_sB_2}=\frac{-(\epsilon_m-\epsilon_s)}{\epsilon_m+\epsilon_s} \quad (2.2.36)$$

$$D_2 = \frac{(\epsilon^+ B_3A_4-\epsilon^+B_4A_2)}{\epsilon^+B_3A_2-\epsilon^-B_2A_3}=\frac{\epsilon_mB_3-\epsilon_mB_4}{\epsilon_mB_3-\epsilon_sB_2}=\frac{2\epsilon_m}{\epsilon_m+\epsilon_s} \quad (2.2.37)$$

$$D_0 = \frac{-\epsilon^+ B_3[\phi]+A_3[\epsilon\phi_x]}{\epsilon^+B_3A_2-\epsilon^-B_2A_3}=\frac{-2\epsilon_mB_3[\phi]+[\epsilon\phi_x]}{\epsilon_mB_3-\epsilon_sB_2}=\frac{-2\epsilon_m[\phi]-h[\epsilon\phi_x]}{\epsilon_m+\epsilon_s} \quad (2.2.38)$$

For $\epsilon_m = 1$, $\epsilon_s = 80$, and $[\phi]$ =0, we have

$$C_1 = \frac{2 \cdot 80}{81}, C_2 = \frac{-79}{81}, C_0 = \frac{-h[\epsilon\phi_x]}{81}, 1 - C_2 = \frac{2 \cdot 80}{81}, \tag{2.2.39}$$

$$D_1 = \frac{79}{81}, D_2 = \frac{2}{81}, D_0 = \frac{-h[\epsilon\phi_x]}{81}, 1 - D_2 = \frac{2}{81}, \tag{2.2.40}$$

which lead to a diagonally dominant matrix from (2.2.30) and (2.2.31). By (2.2.20) and (2.2.21), we introduce two unknows Ψ_{i-1} and Ψ_i in order to treat the two jump condition $[\phi]$ and $[\epsilon\phi]$. If $[\phi] = 0$, we actually have only one jump condition $[\epsilon\phi]$ to take care of. Hence, we should let either $\Psi_i = \phi_i$ or $\Psi_{i-1} = \phi_{i-1}$ in (2.2.21). If we let $\Psi_i = \phi_i$, then (2.2.20) become

$$A_1\phi_{i-1} = A_3\Psi_{i-1} - [\phi] \tag{2.2.41}$$

which means that the fictitious value Ψ_{i-1} will cause an $O(h^2)$ error to approximate $[\phi]$ if (2.2.27) is in use. The next question is from which of (2.2.30) and (2.2.31) we should choose. Numerical results show that (2.2.31) is better. Nevertheless, if both $[\phi] \neq 0$, and $[\epsilon\phi_x] \neq 0$,we should use both.

2.2.3 FDM for Nernst-Planck (NP) equation in primitive form

We first consider the NP equation in the primitive form, and simplify it in 1D as

$$-\frac{\partial J}{\partial x} = \frac{\partial}{\partial x}\left(\left[D\left(\frac{\partial C}{\partial x} + \beta C\frac{\partial \phi}{\partial x}\right)\right]\right) = f = 0. \tag{2.2.42}$$

Differencing (2.2.42) at x_i gives

$$-\frac{\partial J(x_i, y, z)}{\partial x} \approx -\frac{J_{i+\frac{1}{2}} - J_{i-\frac{1}{2}}}{\triangle x} \tag{2.2.43}$$

$$-J_{i+\frac{1}{2}} \approx \left[D\left(\frac{\partial C}{\partial x} + \beta C\frac{\partial \phi}{\partial x}\right)\right]_{i+\frac{1}{2}} \tag{2.2.44}$$

$$\approx \left[D_{i+\frac{1}{2}}\left(\frac{C_{i+1} - C_i}{\triangle x} + \beta_{i+\frac{1}{2}}\frac{C_{i+1} + C_i}{2}\frac{\phi_{i+1} - \phi_i}{\triangle x}\right)\right] \tag{2.2.45}$$

$$-J_{i-\frac{1}{2}} \approx \left[D_{i-\frac{1}{2}}\left(\frac{C_i - C_{i-1}}{\triangle x} + \beta_{i-\frac{1}{2}}\frac{C_i + C_{i-1}}{2}\frac{\phi_i - \phi_{i-1}}{\triangle x}\right)\right] \tag{2.2.46}$$

$$-\frac{\partial J(x_i, y, z)}{\partial x} \approx \frac{1}{\triangle x^2}[a_{i-1}C_{i-1} + a_iC_i + a_{i+1}C_{i+1}] \tag{2.2.47}$$

$$
\begin{aligned}
a_{i-1} &= D_{i-\frac{1}{2}} - D_{i-\frac{1}{2}}\beta_{i-\frac{1}{2}}(\phi_i - \phi_{i-1})/2 && (2.2.48)\\
a_i &= -(D_{i-\frac{1}{2}} + D_{i+\frac{1}{2}}) - D_{i-\frac{1}{2}}\beta_{i-\frac{1}{2}}(\phi_i - \phi_{i-1})/2 && (2.2.49)\\
&\quad + D_{i+\frac{1}{2}}\beta_{i+\frac{1}{2}}(\phi_{i+1} - \phi_i)/2 && (2.2.50)\\
a_{i+1} &= D_{i+\frac{1}{2}} + D_{i+\frac{1}{2}}\beta_{i+\frac{1}{2}}(\phi_{i+1} - \phi_i)/2 && (2.2.51)
\end{aligned}
$$

$$
\frac{a_{i-1}C_{i-1} + a_iC_i + a_{i+1}C_{i+1}}{\triangle x^2} = f_i \qquad (2.2.52)
$$

where equation (2.1.10) is a boundary condition for Nernst-Planck problem not an interface condition. Moreover it is usually called the Robin boundary condition since it involves the data of both the unknown C itself and ∇C. If a boundary condition is in terms of C only, it is then called a Dirichlet boundary condition and is called Neumann boundary condition if in terms of ∇C only. By (2.1.10), we write in 1D as

$$
\begin{aligned}
J \cdot n &= J \cdot \langle 1, 0, 0\rangle = J^x \\
J^x &= -D(\frac{\partial C}{\partial x} + \beta C\frac{\partial \phi}{\partial x}) = g(= 0 \text{ in real equation}) \text{ at } \gamma \qquad (2.2.53)
\end{aligned}
$$

We discuss the finite difference approximation of (2.1.10) in two case.

Case 1. $\mathrm{n} = \langle 1, 0, 0\rangle$, $\mathrm{x}_{i-1} \in \Omega_s$, $\mathrm{x}_i \in \Omega_m$, $\mathrm{x}_{i-\frac{1}{2}} = \gamma$. Let

$$
J^x_{i-\frac{1}{2}} = -\left[D(\frac{\partial C}{\partial x} + \beta C\frac{\partial \phi}{\partial x})\right]_{i-\frac{1}{2}} \qquad (2.2.54)
$$

Finite difference approximation of (2.1.10) at $\mathrm{x}_{i-\frac{1}{2}} = \gamma$ is

$$
\left(-D_{i-\frac{1}{2}}\frac{\Psi_i - C_{i-1}}{\triangle x} - D_{i-\frac{1}{2}}\beta_{i-\frac{1}{2}}\frac{\Psi_i + C_{i-1}}{2}\frac{\phi_i - \phi_{i-1}}{\triangle x}\right) = g_{i-\frac{1}{2}} \qquad (2.2.55)
$$

where Ψ_i is a fictitious value. We extend the function $C(x)$ continuously from x_{i-1} to x_i by considering Ψ_i as an extra unknown that approximates the ghost value $C(x_i)$. This i^{th} FD equation and the $i-1^{th}$ equation (2.2.52) across the interface can be written respectively as

$$
\begin{aligned}
d_i\Psi_i + d_{i-1}C_{i-1} &= \Delta x\ g_{i-\frac{1}{2}} && (2.2.56)\\
\frac{a_{i-2}C_{i-2} + a_{i-1}C_{i-1} + a_i\Psi_i}{\Delta x^2} &= f_{i-1} && (2.2.57)
\end{aligned}
$$

$$
\begin{aligned}
d_i &= -D_{i-\frac{1}{2}} - D_{i-\frac{1}{2}}\beta_{i-\frac{1}{2}}\left(\phi_i - \phi_{i-1}\right)/2 && (2.2.58)\\
d_{i-1} &= D_{i-\frac{1}{2}} - D_{i-\frac{1}{2}}\beta_{i-\frac{1}{2}}\left(\phi_i - \phi_{i-1}\right)/2.
\end{aligned}
$$

Case 2. $\mathbf{n} = \langle -1, 0, 0 \rangle$, $x_i \in \Omega_m$, $x_{i+1} \in \Omega_s$, and $\gamma = x_{i+\frac{1}{2}}$. Similarly, we have

$$d_i \Psi_i + d_{i+1} C_{i+1} = \Delta x \; g_{i+\frac{1}{2}} \tag{2.2.59}$$

$$\frac{a_i \Psi_i + a_{i+1} C_{i+1} + a_{i+2} C_{i+2}}{\Delta x^2} = f_{i+1} \tag{2.2.60}$$

$$\begin{aligned} d_i &= -D_{i+\frac{1}{2}} + D_{i+\frac{1}{2}} \beta_{i+\frac{1}{2}} \left(\phi_{i+1} - \phi_i \right) /2 \\ d_{i+1} &= D_{i+\frac{1}{2}} + D_{i+\frac{1}{2}} \beta_{i+\frac{1}{2}} \left(\phi_{i+1} - \phi_i \right) /2. \end{aligned} \tag{2.2.61}$$

Now we will introducing the Slotoom variable $\widehat{C}_i$ [22] by

$$C_i = \widehat{C}_i \exp(-\beta_i \phi) \tag{2.2.62}$$

the concentration flux is then reformulated to

$$\mathbf{J}_i = -D_i \exp(-\beta_i \phi) \nabla \widehat{C}_i = -\alpha_i \nabla \widehat{C}_i, \;\; \alpha_i = D_i \exp(-\beta_i \phi) \tag{2.2.63}$$

Consequently, the self-adjoint PNP is

$$-\nabla \cdot (\epsilon \nabla \phi) = 4\pi \sum_{j=1}^{N_A} q_j \delta(\mathbf{r} - \mathbf{r}_j) + 4\pi \sum_{i=1}^{2} q_i C_i, \tag{2.2.64}$$

$$-\nabla \cdot \mathbf{J}_i = \nabla \cdot \left[\alpha_i \nabla \widehat{C}_i \right] = 0, \; i = 1, 2 \tag{2.2.65}$$

Consider the Slotboom form of NP (2.2.65) with (2.2.62) and (2.2.63). In 1D, it reads as

$$-\frac{\partial J}{\partial x} = \frac{\partial}{\partial x} \left(\alpha \frac{\partial \widehat{C}}{\partial x} \right) = f \tag{2.2.66}$$

and the FD equation at $x = x_i$ is

$$\frac{\alpha_{i-\frac{1}{2}} \widehat{C}_{i-1} - \left(\alpha_{i+\frac{1}{2}} + \alpha_{i-\frac{1}{2}} \right) \widehat{C}_i + \alpha_{i+\frac{1}{2}} \widehat{C}_{i+1}}{\Delta x^2} = f_i. \tag{2.2.67}$$

Corresponding to (2.2.53) and (2.2.55), we have respectively

$$J^x = -\alpha \frac{\partial \widehat{C}}{\partial x} = g \;\; \text{at } \gamma \tag{2.2.68}$$

$$-\alpha_{i-\frac{1}{2}} \frac{\widehat{\Psi}_i - \widehat{C}_{i-1}}{\Delta x} = g_{i-\frac{1}{2}}, \tag{2.2.69}$$

Eq. (2.2.68) is a Neumann BC. If a Dirichlet BC is considered, we then have

$$\begin{aligned} \widehat{C} &= \widehat{g}_D \ \text{ at } \gamma \Longrightarrow \widehat{\Psi}_i = \widehat{g}_{Di} \text{ or} \\ C &= g_D,\ \Psi_i = g_{Di} \text{ (primitive)}. \end{aligned} \tag{2.2.70}$$

The method (2.2.55) (or (2.2.69)) alone to treat the Robin (or Neumann) BC is usually unstable due to many undefined normal vectors $\mathbf{n}$ at corner points. To stabilize the method, we make connections between the adjacent points of Ψ_i and Ψ_{i-1}. For this, in addition to (2.2.55), we impose

$$\begin{aligned} -\frac{\Psi_i + \Psi_{i-1}}{2} &= -C_{i-\frac{1}{2}} \\ -\Psi_i + \Psi_{i-1} &= 0, \ \text{ if } C_{i-\frac{1}{2}} \text{ is not given.} \end{aligned} \tag{2.2.71}$$

All Robin (with stabilization for the primitive form), Neumann (with stabilization for the Slotboom form), and Dirichlet BCs are implemented for both GA and cylinder. On the interface Γ, we should use either Robin or Neumann BCs. Dirichlet BCs are used only for testing the code. All numerical results are good as shown in the following tables.

2.2.4 The Decomposition of electrostatic potential

We now implement the decomposition method proposed by Chern, Liu, and Wang [5] to cope with the singular charges obtained from the protein data bank (PDB). By this method, the potential $\phi(\mathbf{r})$ is decomposed into

$$\phi(\mathbf{r}) = \widetilde{\phi}(\mathbf{r}) + \overline{\phi}(\mathbf{r}), \ \mathbf{r} \in \overline{\Omega} = \overline{\Omega}_m \cup \overline{\Omega}_s, \ \Gamma = \partial\Omega_m \cap \partial\Omega_s \tag{2.2.72}$$

such that

$$\overline{\phi}(\mathbf{r}) = \begin{cases} \phi^*(\mathbf{r}) + \phi^0(\mathbf{r}), \ \mathbf{r} \in \overline{\Omega}_m \\ 0, \ \mathbf{r} \in \overline{\Omega}_s \backslash \Gamma \end{cases}, \quad \widetilde{\phi}(\mathbf{r}) = \begin{cases} \phi - \phi^* - \phi^0, \ \mathbf{r} \in \overline{\Omega}_m \\ \phi, \ \mathbf{r} \in \overline{\Omega}_s \backslash \Gamma \end{cases} \tag{2.2.73}$$

$$-\nabla \cdot \left(\epsilon \nabla \widetilde{\phi} \right) = 4\pi \sum_{i=1}^{2} q_i C_i, \ \mathbf{r} \in \Omega \backslash \Gamma \tag{2.2.74}$$

$$-\epsilon_m \Delta \overline{\phi} = -\epsilon_m \Delta \phi^* - \epsilon_m \Delta \phi^0, \ \mathbf{r} \in \Omega_m \tag{2.2.75}$$

and the Poission equation of ϕ^0 given by

$$\begin{cases} -\epsilon_m \Delta \phi^0(\mathbf{r}) = 0, \ \mathbf{r} \in \Omega_m \\ \phi^0(\mathbf{r}) = -\phi^*, \ \mathbf{r} \in \partial\Omega_m \end{cases} \tag{2.2.76}$$

and ϕ^* is the Green function given analytically

$$\phi^*(\mathbf{r}) = \sum_{j=1}^{N_A} \frac{q_j}{\epsilon_m \sqrt{(x-x_j)^2+(y-y_j)^2+(z-z_j)^2}}, \ \mathbf{r} \in R^3 \tag{2.2.77}$$

which is the fundamental solution of the following equation

$$-\epsilon_m \Delta \phi^*(\mathbf{r}) = 4\pi \sum_{j=1}^{N_A} q_j \delta(\mathbf{r}-\mathbf{r}_j), \ \mathbf{r} \in R^3. \tag{2.2.78}$$

Summing (2.2.74), (2.2.75), and (2.2.79) gives

$$\begin{aligned} -\nabla \cdot (\epsilon \nabla \phi) &= -\nabla \cdot \left(\epsilon \nabla (\widetilde{\phi} + \overline{\phi})\right) = -\nabla \cdot \left(\epsilon \nabla \widetilde{\phi}\right) - \epsilon_m \Delta \phi^* - \epsilon_m \Delta \phi^0 \\ &= 4\pi \sum_{j=1}^{N_A} q_j \delta(\mathbf{r}-\mathbf{r}_j) + 4\pi \sum_{i=1}^{2} q_i C_i, \ \mathbf{r} \in \Omega \backslash \Gamma. \end{aligned} \tag{2.2.79}$$

which is exactly (2.1.1). Note that ϕ^* satisfies (2.2.79) in the whole space R^3 of a uniform medium with the dielectric constant ϵ_m. Since we have two different media of ϵ_m and ϵ_s in a bounded domain $\overline{\Omega}$, ϕ^0 can be thought as a correction potential to ϕ^* that accounts the electric responses of different dielectrics and boundary conditions. In general, the analytical form of ϕ^0 is not available and hence its numerical approximation is inevitable. We next decompose the interface conditions (2.1.8) and (2.1.9). By (2.2.76) we have

$$\left[\overline{\phi}\right] = 0 \text{ on } \Gamma \tag{2.2.80}$$

which implies that

$$\left[\phi(\mathbf{r})\right] = \left[\widetilde{\phi}\right] + \left[\overline{\phi}\right] = 0, \mathbf{r} \in \Gamma \tag{2.2.81}$$

$$\left[\widetilde{\phi}(\mathbf{r})\right] = 0, \mathbf{r} \in \Gamma \tag{2.2.82}$$

$$\left[\epsilon \phi_{\mathbf{n}}(\mathbf{r})\right] = \left[\epsilon \left(\widetilde{\phi}_{\mathbf{n}} + \overline{\phi}_{\mathbf{n}}\right)\right], \mathbf{r} \in \Gamma \tag{2.2.83}$$

$$\left[\epsilon \widetilde{\phi}_{\mathbf{n}}(\mathbf{r})\right] = \left[\epsilon \phi_{\mathbf{n}}\right] - \left[\epsilon \overline{\phi}_{\mathbf{n}}\right], \mathbf{r} \in \Gamma \tag{2.2.84}$$

$$\left[\epsilon \overline{\phi}_{\mathbf{n}}\right] = \epsilon_m \nabla \left(\phi^* + \phi^0\right) \cdot \mathbf{n}, \mathbf{r} \in \Gamma \tag{2.2.85}$$

$$\begin{aligned} \left[\epsilon \widetilde{\phi}_{\mathbf{n}}(\mathbf{r})\right] &= \left[\epsilon_m \nabla \left(\phi - \phi^* - \phi^0\right) - \epsilon_s \nabla \phi\right] \cdot \mathbf{n}, \mathbf{r} \in \Gamma \\ &= \left[\epsilon_m \nabla \left(-\phi^* - \phi^0\right)\right] \cdot \mathbf{n}, \mathbf{r} \in \Gamma \end{aligned} \tag{2.2.86}$$

due to PNP is three coupled equations and then to introduce iterative method for PNP equations in next section.

2.2.5 The Gummel and SOR-Like schemes

The Gummel algorithm [6] is an outer iteration given by

	Gummel's Algorithm for Nonlinear PNP
step1	Solve (2.2.76) for ϕ^0
step2	Gauss initially $\widetilde{\phi} = \widetilde{\phi}^{(0)}$
step3	Evaluate $\phi = \phi^0 + \widetilde{\phi}^{(0)} + \phi^*$ by (2.2.72)
step4	Solve NP1 $C_1 = C_1^{(0)}$
step5	Solve NP2 $C_2 = C_2^{(0)}$
step6	SOR-Like(2.2.87)
step7	Substitute $C_1^{(0)}$, $C_2^{(0)}$ and solve (2.2.74) for $\widetilde{\phi} = \widetilde{\phi}^{(1)}$
step8	If $\| \widetilde{\phi}^{(1)} - \widetilde{\phi}^{(0)} \|$ or $\| C_i^{(1)} - C_i^{(0)} \|$ >TOL i=1,2 then Go to step3

By [24], the SOR-Like(inner iteration) is a necessary rule for PNP to converge in step6 and is defined as

$$\begin{aligned} \widetilde{\phi}^{new} &= \omega\widetilde{\phi}^{old} + (1-\omega)\widetilde{\phi}^{new} \\ C_i^{new} &= \omega C_i^{old} + (1-\omega)C_i^{new} \end{aligned} \tag{2.2.87}$$

where the relaxation parameter ω is selected between 0 and 2.

2.3 Test case for PNP equations

Now we will check the method described above can achieve quadratic convergence. For nonlinear PNP models, the test solutions [24] are chosen to be

$$\widetilde{\phi}(\mathbf{r}) = \cos x \cos y \cos z,\ \mathbf{r} \in \Omega \tag{2.3.1}$$

$$\phi(\mathbf{r}) = \begin{cases} \widetilde{\phi}(\mathbf{r}) + \phi^0(\mathbf{r}) + \phi^*(\mathbf{r}), & \mathbf{r} \in \Omega_m \\ \widetilde{\phi}(\mathbf{r}), & \mathbf{r} \in \Omega_s \end{cases} \tag{2.3.2}$$

$$C_1(\mathbf{r}) = \begin{cases} 0, & \mathbf{r} \in \Omega_m \\ 0.2\cos x \cos y \cos z + 0.3, & \mathbf{r} \in \Omega_s \end{cases} \tag{2.3.3}$$

$$C_2(\mathbf{r}) = \begin{cases} 0, & \mathbf{r} \in \Omega_m \\ 0.1\cos x \cos y \cos z + 0.3, & \mathbf{r} \in \Omega_s \end{cases} \tag{2.3.4}$$

where $r = (x, y, z)$ and the PNP system can be written in the following form

$$\mathrm{P}^0 \quad : \quad \begin{cases} -\epsilon_m \Delta\phi^0(\mathbf{r}) = 0, & \mathbf{r} \in \Omega_m \\ \phi^0(\mathbf{r}) = -\phi^*(\mathbf{r}) \ , & \mathbf{r} \in \partial\Omega_m \end{cases} \tag{2.3.5}$$

$$\mathrm{P} \quad : \quad -\nabla \cdot (\epsilon(\mathbf{r})\nabla\widetilde{\phi}(\mathbf{r})) = \sum_{i=1}^{2} q_i C_i(\mathbf{r}) + F(\mathbf{r}), \mathbf{r} \in \Omega \tag{2.3.6}$$

$$\mathrm{NP1} \quad : \quad -\nabla \cdot J_1(\mathbf{r}) = F_1, \ \mathbf{r} \in \Omega_s \tag{2.3.3}$$

$$\mathrm{NP2} \quad : \quad -\nabla \cdot J_2(\mathbf{r}) = F_2, \ \mathbf{r} \in \Omega_s \tag{2.3.4}$$

$$J_i(\mathbf{r}) = -D_i(\mathbf{r}) \left[\nabla C_i(\mathbf{r}) + q_i C_i(\mathbf{r}) \nabla\phi(\mathbf{r})\right], i = 1.2 \tag{2.3.5}$$

$$\phi^*(\mathbf{r}) = \sum_{j=1}^{N_A} \frac{q_j}{\epsilon_m \sqrt{(x-x_j)^2 + (y-y_j)^2 + (z-z_j)^2}}, \mathbf{r} \in \Omega_m \tag{2.3.6}$$

where $q_1 = 1$, $q_2 = -1$, $D_1 = D_2 = 1$, and the right hand side can be calculated as the following

$$F(\mathbf{r}) = \begin{cases} (3\epsilon_s\text{-}0.1)\cos\mathrm{x}\cos\mathrm{y}\cos\mathrm{z}, \mathbf{r} \in \Omega_s \\ 3\epsilon_m \cos\mathrm{x}\cos\mathrm{y}\cos\mathrm{z}, \mathbf{r} \in \Omega_m \end{cases}, \epsilon_m = 1, \ \epsilon_s = 80 \tag{2.3.7}$$

$$F_1(\mathbf{r}) = \nabla \cdot \left[\nabla C_1(\mathbf{r}) + C_1(\mathbf{r})\nabla\widetilde{\phi}(\mathbf{r})\right], \ \mathbf{r} \in \Omega_s \tag{2.3.8}$$

$$F_2(\mathbf{r}) = \nabla \cdot \left[\nabla C_2(\mathbf{r}) - C_2(\mathbf{r})\nabla\widetilde{\phi}(\mathbf{r})\right], \mathbf{r} \in \Omega_s \tag{2.3.9}$$

For the test case, we have three unknown $C_1(\mathbf{r})$, $C_2(\mathbf{r})$ and $\widetilde{\phi}(\mathbf{r})$. Due to we decompose the electrostatic potential ϕ, and thus avoid the problem of delta function. On interface Γ, the jump condition are given by

$$[\epsilon\phi_n] = (\epsilon_m \nabla(\widetilde{\phi} + \phi^0 + \phi^*) - \epsilon_s \nabla\widetilde{\phi}) \cdot \mathbf{n} \neq 0 \text{ and } [\phi] = 0 \tag{2.3.10}$$

then we have two jump condition of $\widetilde{\phi}$ as following

$$[\widetilde{\phi}] = 0 \tag{2.3.11}$$

$$[\epsilon\widetilde{\phi}_n] = (\epsilon_m \nabla\widetilde{\phi} - \epsilon_s \nabla\widetilde{\phi}) \cdot \mathbf{n} = (\epsilon_m \nabla \cos x \cos y \cos z - \epsilon_s \nabla \cos x \cos y \cos z) \cdot \mathbf{n} \tag{2.3.12}$$

3 The Poisson-Boltzmann (PB) equation

The PB equation is to describe the electrostatic potential of the ion concentration in the uniform state. For the solution of the PB equation, we put this process into two

steps. First,we use finite difference to solve the linearized PB equation and initial guess of nonlinear PB equation are obtained. Second, when we get a good initial guess, we will need to implement monotone iterative method [17] for our nonlinear PB equation.

3.1 The Poisson-Boltzmann (PB) equation and linearization

Because PNP models are nonlinear and coupled with C_1, C_2 and ϕ, the initial guess of $\tilde{\phi}^0$ is a function that must be carefully computed. After reading Appendix 2 in [23], we realized that the initial guess function should be set as the solution of the Poisson-Boltzmann (PB) equation

$$-\nabla \cdot (\epsilon(r)\nabla\phi(r)) = 4\pi \sum_{j=1}^{N_A} q_j \delta(r - r_j) + 4\pi \sum_{i=1}^{2} q_i C_i^{bulk} \exp(-\beta_i \phi(r)),\ r \in \Omega \qquad (3.1.1)$$

where C^{Bulk} is bulk concentration of mobile ions of ith type are given and other parameter are same with (2.1.1). We will need to implement monotone iterative method [17] for both nonlinear PB and PNP models. An electrolyte is any substance containing free ions that make the substance electrically conductive. Electrolyte solutions are normally formed when a salt (NaCl) is placed into a solvent such as water and the individual components dissociate due to the thermodynamic interactions between solvent (water) and solute molecules (NaCl), in a process called solvation. This redistribution of solute molecules in solvent is the focus of Debye-Huckel theory. This theory uses the Boltzmann factor $\exp(-\beta_i\phi(r))$ of dissolved ions with q_i in the local electrostatic potential $\phi(r)$ to estimate the increase or dicrease in the local concetration $C_i(r)$ relative their bulk concentration $C_i^{bulk}(r)$, i,e.,

$$C_i(r) = C_i^{bulk}(r) \exp(-\beta_i \phi(r)) \qquad (3.1.2)$$

Of course, the potential $\phi(r)$ is itself influenced by the redistribution of sodium (Na) and chloride (Cl) and by the location of singular charges q_j, so the potentials and concentrations must be solved for self-consistently. The bulk concentration $C_i^{bulk}(r)$ is defined the ratio of the total number of mobile ions of i^{th} type and the total volume that they occupy. It is zero inside the solute and constant outside. The PNP model (2.1.1)-(2.1.3) reduces to the PB model in the absence of a flux, i.e., in the absence of applied voltage, i.e., $V_0 = 0$ in dirichlet boundary condition. The PB equation is usually applied to a 1:1 salt solution where there are cations (positive charges) of valence z with a counter ion

(negative) of valence $-z$. In this case with $z = 1$, we have $C_i^{bulk}(r) = C_0$ and

$$\begin{aligned}
\sum_{i=1}^{2} q_i C_i^{bulk} \exp(-\beta_i \phi(r)) &= e_c C_1^{bulk} \exp(-\beta_1 \phi(r)) - e_c C_2^{bulk} \exp(-\beta_2 \phi(r)) \\
&= 2e_c C_0 \frac{\exp(-\beta_1 \phi(r)) - \exp(-\beta_2 \phi(r))}{2} \\
&= 2e_c C_0 \frac{\exp(-\frac{e_c}{K_B T}\phi(r)) - \exp(\frac{e_c}{K_B T}\phi(r))}{2} \\
&= -2e_c C_0 \sinh(\frac{e_c}{K_B T}\phi(r)) \\
&= -\frac{2e_c^2 C_0}{K_B T}\frac{K_B T}{e_c} \sinh(\frac{e_c}{K_B T}\phi(r)) \\
&= -k^2 \frac{K_B T}{e_c} \sinh(\frac{e_c}{K_B T}\phi(r)) \qquad (3.1.3)
\end{aligned}$$

where

$$k^2 = \begin{cases} \frac{2e^2 C_0}{K_B T}, & r \in \Omega_s \\ 0, & r \in \Omega_m \end{cases}$$

The nonlinear PB equation is thus

$$-\nabla \cdot (\epsilon(r)\nabla\phi(r)) + 4\pi k^2 \frac{K_B T}{e_c} \sinh(\frac{e_c}{K_B T}\phi(r)) = 4\pi \sum_{j=1}^{N_A} q_j \delta(r - r_j), \ r \in \Omega \qquad (3.1.4)$$

Applying Taylor's expansion

$$e^\theta = 1 + \frac{\theta}{1!} + \frac{\theta^2}{2!} + \frac{\theta^3}{3!} + ... \qquad (3.1.5)$$

to $\sinh(\frac{e_c}{K_B T}\phi(r))$ with $\theta = \frac{e_c}{K_B T}\phi(r)$, we obtain

$$\sinh(\frac{e_c}{K_B T}\phi(r)) = \theta + \frac{\theta^3}{6} + ... \qquad (3.1.6)$$

The linearized PB equation corresponds to the first degree approximation of Taylor's expansion, i.e., $\sinh(\frac{e}{K_B T}\phi(r)) \approx \theta$ and is written as

$$\begin{aligned}
-\nabla \cdot (\epsilon(r)\nabla\phi(r)) + 4\pi k^2 \frac{K_B T}{e}\theta &= -\nabla \cdot (\epsilon(r)\nabla\phi(r)) + 4\pi k^2 \phi(r) \\
&= 4\pi \sum_{j=1}^{N_A} q_j \delta(r - r_j), \ r \in \Omega \qquad (3.1.7)
\end{aligned}$$

Because of delta functions and using the decomposition method previously described, (3.1.1) can be written as

$$\begin{aligned} -\nabla\cdot(\epsilon(r)\nabla\phi(r)) &= -\nabla\cdot(\epsilon(r)\nabla\widetilde{\phi}(r)) - \epsilon_m\Delta\phi^* - \epsilon_m\Delta\phi^0 \\ &= 4\pi\sum_{j=1}^{N_A} q_j\delta(r-r_j) + 4\pi\sum_{i=1}^{2} q_i C_i^{bulk}\exp(-\beta_i(\overline{\phi}+\widetilde{\phi})) \end{aligned} \tag{3.1.8}$$

which yields, in corresponding to (2.2.74),

$$\begin{aligned} -\nabla\cdot(\epsilon(r)\nabla\widetilde{\phi}(r)) &= 4\pi\sum_{i=1}^{2} q_i C_i^{bulk}\exp(-\beta_i(\overline{\phi}+\widetilde{\phi})) \\ &= 4\pi\sum_{i=1}^{2} q_i C_i^{bulk}\exp(-\beta_i\widetilde{\phi}) \qquad (3.1.9) \\ C^{bulk} &= \begin{cases} 0, & r\in\Omega_m \\ \text{constant}, & r\in\Omega_s \end{cases} \end{aligned}$$

Similarly, for (3.1.4) and (3.1.7), we have

$$-\nabla\cdot(\epsilon(r)\nabla\widetilde{\phi}(r)) + 4\pi k^2\frac{K_BT}{e_c}\sinh(\frac{e_c}{K_BT}\widetilde{\phi}(r)) = 0,\ r\in\Omega/\Gamma \tag{3.1.10}$$

$$-\nabla\cdot(\epsilon(r)\nabla\widetilde{\phi}(r)) + 4\pi k^2\widetilde{\phi}(r) = 0,\ r\in\Omega/\Gamma \tag{3.1.11}$$

with

$$k^2 = \begin{cases} \frac{2e_c^2C_0}{K_BT}, & r\in\Omega_s \\ 0, & r\in\Omega_m \end{cases} \tag{3.1.12}$$

The boundary and interface conditions for $\widetilde{\phi}$ are the same as those in (2.2.80) (2.2.86).

3.2 Monotone iterative method for the nonlinear PB equation

Discretization of the left hand side of linear PB equation (3.1.11) by the central finite difference method (FDM) yields

$$\begin{aligned} -\frac{\partial}{\partial x}\left(\epsilon(\mathbf{r})\frac{\partial\widetilde{\phi}(x_i,y,z)}{\partial x}\right) + 4\pi k^2\widetilde{\phi}(x_i,y,z) &\approx \\ \frac{-\epsilon_{i-\frac{1}{2}}\widetilde{\phi}_{i-1} + \left[\left(\epsilon_{i-\frac{1}{2}}+\epsilon_{i+\frac{1}{2}}\right) + 4\pi k^2\Delta x^2\right]\widetilde{\phi}_i - \epsilon_{i+\frac{1}{2}}\widetilde{\phi}_{i+1}}{\Delta x^2}, & r \in \Omega\backslash\Gamma \end{aligned} \tag{3.2.1}$$

with

$$k^2 = \begin{cases} \frac{2e_c^2C_0}{K_BT}, & r\in\Omega_s \\ 0, & r\in\Omega_m \end{cases} \tag{3.2.2}$$

and for the interface condition, we use the MIB method (2.2.32). Now back to the nonlinear PB equation (3.1.10). Let

$$F(\widetilde{\phi}) = 4\pi k^2 \frac{K_B T}{e_c} \sinh(\frac{e_c}{K_B T}\widetilde{\phi}(r)),\ r \in \Omega\backslash\Gamma \tag{3.2.3}$$

$$G(\widetilde{\phi}) = -\nabla\cdot(\epsilon(r)\nabla\widetilde{\phi}(r)) + 4\pi k^2 \frac{K_B T}{e_c} \sinh(\frac{e_c}{K_B T}\widetilde{\phi}(r)),\ r \in \Omega\backslash\Gamma \tag{3.2.4}$$

Define

$$\begin{aligned} G'(\widetilde{\phi})\omega &: = \lim_{t->0} \frac{G(\widetilde{\phi}+t\omega) - G(\widetilde{\phi})}{t} \\ &= \lim_{t->0} \frac{-\nabla\cdot(\epsilon(r)\nabla(\widetilde{\phi}(r)+t\omega)) + F(\widetilde{\phi}+t\omega) + \nabla\cdot(\epsilon(r)\nabla\widetilde{\phi}(r)) - F(\widetilde{\phi})}{t} \\ &= \lim_{t->0} \frac{-\nabla\cdot(\epsilon(r)\nabla(t\omega)) + F(\widetilde{\phi}+t\omega) - F(\widetilde{\phi})}{t} \\ &= -\nabla\cdot(\epsilon(r)\nabla\omega) + \omega F'(\widetilde{\phi}) \end{aligned} \tag{3.2.5}$$

Note that the differentiations in $-\nabla\cdot(\epsilon(r)\nabla\omega)$ and $F'(\widetilde{\phi})$ are different, i.e., $\nabla\omega = (\frac{\partial\omega}{\partial x}, \frac{\partial\omega}{\partial y}, \frac{\partial\omega}{\partial z})$ and $F'(\widetilde{\phi}) = \frac{dF(\widetilde{\phi})}{d\widetilde{\phi}}$ etc. The linearized problem of (3.1.10) is thus

$$G'(\widetilde{\phi}^{(0)})\omega = -\nabla\cdot(\epsilon(r)\nabla\omega) + \omega F'(\widetilde{\phi}^{(0)}) = G(\widetilde{\phi}^{(0)}),\ \omega = \widetilde{\phi}^{(0)} - \widetilde{\phi}^{(1)} \tag{3.2.6}$$

then we have

$$\nabla\cdot(\epsilon(r)\nabla\widetilde{\phi}^{1}) - F'(\widetilde{\phi}^{(0)})\widetilde{\phi}^{(1)} = F(\widetilde{\phi}^{(0)}) - F'(\widetilde{\phi}^{(0)})\widetilde{\phi}^{(0)} \tag{3.2.7}$$

$$[A - F'(\widetilde{\phi}^{(0)})]\widetilde{\phi}^{(1)} = F(\widetilde{\phi}^{(0)}) - F'(\widetilde{\phi}^{(0)})\widetilde{\phi}^{(0)} \tag{3.2.8}$$

where A is a coefficient matrix corresponding to the discretization of $\nabla\cdot(\epsilon(r)\nabla\widetilde{\phi}^{(1)})$, $F'(\widetilde{\phi}^{(0)})$ is a diagonal matrix with entries $d_{ii} = F'(\widetilde{\phi}^{(0)}(r_i))$ with $\widetilde{\phi}^{(0)}(r_i) =: \widetilde{\phi}_i^{(0)} \approx \widetilde{\phi}(r_i)$, $\widetilde{\phi}^{(0)}$ are obtained by linear PB.

The monotone iterative method with FDM for (3.1.10) is to replace (3.2.9) by more general form

$$[A - \Lambda]\widetilde{\phi}^{(1)} = -\Lambda\widetilde{\phi}^{(0)} + F(\widetilde{\phi}^{(0)}) \tag{3.2.9}$$

where Λ can be a constant diagonal matrix or a variable diagonal matrix. Of course if $\Lambda = F'(\widetilde{\phi}^{(0)})$, we have Newton's method. The MIB method is once again be used on interface Γ.

4 Dimensionless formulation and approximation of interface condition

4.1 Unit Conversion and physical constants

For real physical problems, It is important to solve PB and coupled PNP equations in one unit convention. We apply the Gaussian units shown in following tables and the dimensionless process show in next section.

Table 4.1. Physical Constants

Symbol	Meaning	Value	Unit	Reference
Å	Angstrom	10^{-8}	cm	
A	ampere	1A = 1 C/s	A	
cal	calorie	4.1859×10^{7}	erg	
C	coulomb	$10^{10}/3.336$	esu	
D_{K^+}	diffusion coefficient	2×10^{-5}	cm^2/s	[24]
D_{Cl^-}	diffusion coefficient	2.03×10^{-5}	cm^2/s	[24]
$e = e_{\mathrm{c}}$	elementary (proton) charge	4.8032424×10^{-10}	esu	
ϵ_r	dielectric constant		no unit	
ϵ_0	vacuum permittivity	8.8542×10^{-12}	$\mathrm{Cm}^{-1}\mathrm{V}^{-1}$	
h	Planck's constant	6.6261×10^{-34}	J s	
I	current		A	
J	joule	10^{7}	erg	
k_{B}	Boltzmann constant	1.3807×10^{-16}	erg/K	
l	liter (volume)		cm^3	
M	molar (moles per liter)		$\mathrm{mol}/\mathrm{cm}^3$	
mol		6.0221×10^{23}		
$\mathrm{N_A}$	Avagadro's number	6.0221×10^{23}	mol^{-1}	
T	temperature	273.15 + T (^{o}C)	K	
V	volt	3.336×10^{-3}	erg/esu	

Table 4.2.Unit Scale Factors

Name	femto	pico	nano	micro	milli	centi	deci	kilo	mega	giga
Prefix	f	p	n	μ	m	c	d	k	M	G
Factor	10^{-15}	10^{-12}	10^{-9}	10^{-6}	10^{-3}	10^{-2}	10^{-1}	10^{3}	10^{6}	10^{9}

Table 4.3. Unit Convention				
Meaning	Symbol	Value	Unit	Ref.
Potential	$k_{\mathrm{B}}T/e_c$	$=1.3807\times10^{-16}\times300/(4.8032424\times10^{-10})$ $=8.62355\times10^{-5}$	erg/esu	
Concentration	M=molar	= mol/l $=6.0221\times10^{23}/\mathrm{cm}^3$	cm^{-3}	
Current	pA	= pico ampere $=10^{-12}$	A	

Table 4.4. Gaussian units[24]				
abbr	unit	represents	equivalent expressions	
dyn	dyne	force	$\mathrm{esu}^2/\mathrm{cm}^2$	
erg	erg	energy	dyn·cm	

4.2 Dimensionless formulation

Physical phenomena within a channel system are controlled by boundary conditions (BCs). We now describe the BCs of the PNP system. For the Poisson equation (2.1.1), the voltage applied to the system is given by the potential difference (a Dirichlet BC), denoted by $V_0 > 0$ and shown in Fig. 4, along the z direction, and a Neumann BC on other parts of $\partial\Omega$, namely,

$$\begin{aligned} \phi\left(x,y,0\text{Å}\right) &= V_0,\ \phi\left(x,y,40\text{Å}\right)=0 && (4.1)\\ \frac{\partial\phi}{\partial\mathbf{n}} &= 0, \text{ for } |x|=20 \text{ or } |y|=20 \text{ and } z\neq 40 \text{ and } 0. && (4.1(a)) \end{aligned}$$

The unit of V_0 is mV (milli volt). The boundary data for C_i is similarly denoted by C_0 in the unit of M (molar). Moreover, a single value of C_0 is assumed for both $C_1(x,y,z)$ and $C_2(x,y,z)$ on $\partial\Omega\cap\partial\Omega_s$, i.e.,

$$C_1(x,y,z)=C_2(x,y,z)=C_0,\ \ \forall\,(x,y,z)\in\partial\Omega\cap\partial\Omega_s. \tag{4.2}$$

For this project, the dielectric constants are set to

$$\epsilon_m=2,\epsilon_s=80 \tag{4.3}$$

and the diffusion coefficients in bulk are given in Table 4.1. Note that the Gaussian units are adopted in [24]. The fundamental difference between the SI (International System of Units) and Gaussian units lies in the presentation of Coulomb's law

$$F=\frac{q_1q_2}{4\pi\epsilon_0r^2}\ [\text{SI}]=\frac{q_1q_2}{r^2}\ [\text{CGS-Gaussian}], \tag{4.4}$$

where CGS stands for centimetre-gram-second. Note that the vacuum permittivity ϵ_0 does not appear in the Gaussian format (in [24]).

Let $l = 1\text{Å}(10^{-8}cm)$. By using the following scalings with the new dimensionless quantities marked by the subscript (or supscript)

$$x_s = \frac{x}{l}, \quad y_s = \frac{y}{l}, \quad z_s = \frac{z}{l} \tag{4.5}$$

$$\widetilde{\phi}^s = \widetilde{\phi}\frac{e_c}{k_{\mathrm{B}}T},\ q_i^s = \frac{q_i}{e_c},\ C_i^s = C_i\frac{l^2e_c^2}{k_{\mathrm{B}}T},\ D_i^s = \frac{D_i}{l^2} \tag{4.6}$$

Eq. (2.2.74) can be written as

$$\begin{aligned} -\nabla_s\cdot\left(\frac{\epsilon_r k_{\mathrm{B}}T}{l^2e_c}\nabla_s\widetilde{\phi}^s\right) &= \sum_{i=1}^{2} q_iC_i \\ -\nabla_s\cdot\left(\epsilon_r\nabla_s\widetilde{\phi}^s\right) &= \sum_{i=1}^{2}\frac{q_i}{e_c}C_i\frac{l^2e_c^2}{k_{\mathrm{B}}T} = \sum_{i=1}^{2} q_i^sC_i^s \end{aligned} \tag{4.7}$$

where $\nabla_s = \left\langle \frac{\partial}{\partial x_s}, \frac{\partial}{\partial y_s}, \frac{\partial}{\partial z_s}\right\rangle$. And (2.1.2) and (2.1.3) can be expressed as

$$\begin{aligned} \frac{1}{l^2}\nabla_s\cdot D_i\left[\nabla_sC_i + \frac{k_{\mathrm{B}}T}{e_c}\frac{q_i}{k_{\mathrm{B}}T}C_i\nabla_s\phi^s\right] &= 0 \\ \frac{1}{l^2}\nabla_s\cdot D_i\left[\nabla_sC_i + q_i^sC_i\nabla_s\phi^s\right] &= 0 \\ \frac{k_{\mathrm{B}}T}{l^2e_c^2}\nabla_s\cdot D_i^s\left[\nabla_sC_i^s + q_i^sC_i^s\nabla_s\phi^s\right] &= 0 \\ \nabla_s\cdot D_i^s\left[\nabla_sC_i^s + q_i^sC_i^s\nabla_s\phi^s\right] &= 0 \end{aligned} \tag{4.8}$$

We further check the unit of C_i^s that

$$\begin{aligned} C_i^s = \frac{C_il^2e_c^2}{k_{\mathrm{B}}T} &= \frac{6.0221\times10^{23}\times10^{-16}\times(4.8032424)^2\times10^{-20}}{1.3806620\times10^{-16}\times300} \\ &= 335.4257\ \left[\frac{\mathrm{cm^2esu^2}}{\mathrm{cm^3\cdot erg}} = \frac{\mathrm{esu^2}}{\mathrm{esu^2}}\ (\text{no unit})\right]. \end{aligned} \tag{4.9(a)}$$

$$\begin{aligned} \widetilde{\phi}^s &= \widetilde{\phi}\frac{e_c}{k_{\mathrm{B}}T} \\ &= \frac{4.8032424\times10^{-10}}{300\times1.3806620\times10^{-16}}\ \left[\frac{\text{V esu}}{\text{erg}} = \frac{\frac{\text{J}}{\text{C}}\text{esu}}{\text{erg}} = \frac{\text{J esu}}{\text{C erg}} = \frac{10^7\text{erg esu}}{\frac{10^{10}}{3.336}\text{esu erg}}\right] \\ &= \frac{4.8032424\times10^{-10}}{300\times1.3806620\times10^{-16}}\cdot\frac{10^7}{\frac{10^{10}}{3.336}}\left[\frac{\text{erg esu}}{\text{esu erg}}(\text{no unit})\right] \\ &= 38.6858\,[(\text{no unit})] \end{aligned} \tag{4.9(b)}$$

Moreover, we verify a similar unit defined in [24] using its notation (see Eq. (52) in [24] where 1 dyne = esu^2/cm should be 1 dyne = esu^2/cm in Table 5)

$$\begin{aligned}
\frac{k_{\mathrm{B}}T}{e_{\mathrm{c}}} &= \frac{1.380662\times10^{-16}\times300}{4.8032424\times10^{-10}}\ \left[\frac{\text{dyn cm}}{\text{esu}}=\frac{\text{esu}^2}{\text{esu}}=\frac{\text{esu}}{\text{cm}}\right] \qquad (4.10)\\
&= 0.8623\times10^{-4}\ \left[\frac{\text{esu}}{\text{cm}}\right]\\
1\,[\text{dyn}] &= 1\left[\frac{\text{g cm}}{\text{s}^2}\right]=10^{-5}\ [\text{N}]\,,\quad 1\,[\text{esu}]=1\left[\text{dyn}^{1/2}\text{cm}\right]\\
1\,[\text{erg}] &= 1\,[\text{dyn}\cdot\text{cm}]=10^{-7}\ [\text{J}]\,,\quad \text{J}=\frac{\text{kg}\cdot\text{m}^2}{\text{s}^2}=\text{N}\cdot\text{m}\\
1\,[\text{esu}] &= 3.336\times10^{-10}\ [\text{C}] \qquad (4.11)
\end{aligned}$$

$$\begin{aligned}
u_{bd} &= \widetilde{\Phi}_{bd}\frac{e_c}{300\times k_{\mathrm{B}}T}=\widetilde{\Phi}_{bd}\frac{1}{300\cdot0.8623\times10^{-4}}=38.6563\widetilde{\Phi}_{bd} \qquad (4.12a)\\
200\text{mV}\frac{e_c}{300k_{\mathrm{B}}T} &= 0.02580\,[\text{ no unit (by (4.9(b)))}]\\
\widetilde{C}_{bd} &= C_{bd}\frac{\mathrm{N_A}l^2e_{\mathrm{c}}^2}{10^3k_{\mathrm{B}}T}=C_{bd}\frac{6.0221\times10^{23}\times10^{-16}\ \times(4.8032424\times10^{-10})}{10^3\times0.8623\times10^{-4}}\\
&= 0.33545C_{bd}\ \ [\text{no unit (by (4.9(a)))}] \qquad (4.12b)\\
\frac{\widetilde{C}_{bd}}{u_{bd}} &= 0.0008677\frac{C_{bd}}{\widetilde{\Phi}_{bd}}
\end{aligned}$$

From above relations, we observe that the Gaussian units are quite complicated and that the scaled concentration (4.7) and (4.8) is dimensionless. We will use the CGS-Gaussian units.

Remark 4.1. The above scaling convention is used in our code. For example, the coordinate system of the domain is expressed by (4.5) and the dielectric constants are exactly given as (4.3). Consequently, the BC (4.1) is also required to be scaled as

$$V_0^s=V_0\frac{e}{k_{\mathrm{B}}T}=38.6858\times\frac{1}{10^3}=0.0386858\ \left[\frac{\text{V}}{\text{V}}\ (\text{no unit})\right]. \qquad (4.13)$$

We thus have

$$V_0=100\text{mV}\Longrightarrow V_0^s=3.86858. \qquad (4.14)$$

Similarly, for (4.2), we have by (4.9(a))

$$C_0=1\text{M (molar)}\Longrightarrow C_0^s=335.4257 \qquad (4.15)$$

Note that we can scale Eq. (4.8) further as

$$\frac{(4.8)}{100}\Longrightarrow\frac{C_0^s}{100}=3.354257 \qquad (4.16)$$

Moreover, we also have

$$\begin{aligned} q^s_{\mathrm{K}^+} &= 1,\ q^s_{\mathrm{Cl}^-} = -1, \\ D^s_{\mathrm{K}^+} &= \frac{2\times 10^{-5}}{10^{-16}}\left[\frac{\mathrm{cm}^2}{\mathrm{cm}^2\ \mathrm{s}}\right] = 2\times 10^{11}\left[\frac{1}{\mathrm{s}}\right] \\ D^s_{\mathrm{Cl}^-} &= \frac{2\times 10^{-5}}{10^{-16}}\left[\frac{\mathrm{cm}^2}{\mathrm{cm}^2\ \mathrm{s}}\right] = 2.03\times 10^{11}\left[\frac{1}{\mathrm{s}}\right] \\ \frac{(4.8)}{10^{11}} &\Longrightarrow \frac{D^s_{\mathrm{K}^+}}{10^{11}} = 2,\ \frac{D^s_{\mathrm{Cl}^-}}{10^{11}} = 2.03. \end{aligned} \tag{4.17}$$

Remark 4.2. Following [24], the diffusion coefficient profiles are defined via an interpolation function along the z-axis (the channel axis)

$$f(\mathbf{r}) = f(z) = n\left(\frac{z-z_{\mathrm{ch}}}{z_{\mathrm{bu}}-z_{\mathrm{ch}}}\right)^{n+1} - (n+1)\left(\frac{z-z_{\mathrm{ch}}}{z_{\mathrm{bu}}-z_{\mathrm{ch}}}\right)^{n} \tag{4.18}$$

where $n \geq 2$ is an integer, $z \in [z_{\mathrm{ch}}, z_{\mathrm{bu}}]$ which is a buffering region between the channel pore and bulk regions. The diffusion coefficient function is then defined by

$$D(\mathbf{r}) = \begin{cases} D_{\mathrm{ch}} & \mathbf{r} \in \text{Channel region} \\ D_{\mathrm{ch}} + (D_{\mathrm{ch}} - D_{\mathrm{bu}})f(\mathbf{r}) & \mathbf{r} \in \text{Buffering region} \\ D_{\mathrm{bu}} & \mathbf{r} \in \text{Bulk region} \end{cases} \tag{4.19}$$

$$D_{\mathrm{bu}} = D_{\mathrm{K}^+} \text{ or } D_{\mathrm{bu}} = D_{\mathrm{Cl}^-} \text{ and } D_{\mathrm{ch}} = 0.05 D_{\mathrm{bu}}. \tag{4.20}$$

The buffering region is set (symmetrically about $z=0$) to

$$\begin{aligned} z_{\mathrm{bu}} - z_{\mathrm{ch}} &= \frac{55}{9}\text{Å}\ ,\ z_{\mathrm{bu}} = 13\text{Å},\ \text{if } n = 2 \\ z_{\mathrm{bu}} - z_{\mathrm{ch}} &= \frac{35}{9}\text{Å}\ ,\ z_{\mathrm{bu}} = 13\text{Å},\ \text{if } n = 9 \\ z_{\mathrm{bu}} - z_{\mathrm{ch}} &= \frac{20}{9}\text{Å}\ ,\ z_{\mathrm{bu}} = 13\text{Å},\ \text{if } n = 19. \end{aligned} \tag{4.21}$$

Example 4.1. Nonlinear GA PNP, Singualr Charges, Diffusion Function (4.19), no Exact Solutions. We now try to reproduce the results of Figure 9 and Table 6 in [24]. The BC data for this case are as follows:

$$V_0 = 200\text{mV},\ C_0 = 0.1\text{M} \Longrightarrow V_0^s = 7.73716,\ C_0^s = 33.54257 \tag{4.22}$$

The first thing needed attention is scaling. From above dimensionless analysis, the orders of (4.14) and (4.15) are $O(1)$ and $O(10^2)$, respectively. The code will blow up if (4.16) is not used. Therefore, the scaled variables $\widetilde{\phi}^s$ and C_i^s in (4.6) should be changed to

$$\widetilde{\phi}^s = \widetilde{\phi}\frac{e_c}{\omega_1 k_{\mathrm{B}} T},\ C_i^s = C_i\frac{l^2 e_c^2}{\omega_2 k_{\mathrm{B}} T},\ V_0^s = \frac{7.73716}{\omega_1},\ C_0^s = \frac{33.54257}{\omega_2} \tag{4.23}$$

where the scaling factors ω_1 and ω_2 are crucial for the convergence behavior of Gummel's algorithm and will be chosen from the coding experience. Accordingly, (2.2.79) should be scaled as follows

$$\begin{aligned} -\nabla\cdot(\epsilon_r\nabla\phi) &= -\nabla\cdot\left(\epsilon_r\nabla(\widetilde{\phi}+\overline{\phi})\right) \\ &= -\left(\frac{\omega_1 k_{\mathrm{B}}T}{l^2 e}\right)\left[\nabla_s\cdot\left(\epsilon_r\nabla_s\widetilde{\phi}^s\right)+\epsilon_m\Delta_s\phi_s^*+\epsilon_m\Delta_s\phi_s^0\right] \\ &= 4\pi\sum_{j=1}^{N_A}q_j\delta(\mathbf{r}-\mathbf{r}_j)+4\pi\sum_{i=1}^{2}q_iC_i \end{aligned} \tag{4.24}$$

$$\begin{aligned} &-\left[\nabla_s\cdot\left(\epsilon_r\nabla_s\widetilde{\phi}^s\right)+\epsilon_m\Delta_s\phi_s^*+\epsilon_m\Delta_s\phi_s^0\right] \\ &=\left(\frac{l^2e_c}{\omega_1 k_{\mathrm{B}}T}\right)\left[4\pi\sum_{j=1}^{N_A}q_j\delta(\mathbf{r}-\mathbf{r}_j)+4\pi\sum_{i=1}^{2}q_iC_i\right] \\ &=4\pi\sum_{j=1}^{N_A}\frac{q_j}{e_c}\delta(\mathbf{r}-\mathbf{r}_j)\frac{l^2e_c^2}{\omega_1 k_{\mathrm{B}}T}+4\pi\sum_{i=1}^{2}\frac{q_i}{e_c}C_i\frac{l^2e_c^2}{\omega_1 k_{\mathrm{B}}T} \\ &=4\pi\sum_{j=1}^{N_A}q_j^s\delta_s(\mathbf{r}^s-\mathbf{r}_j^s)+4\pi\frac{\omega_2}{\omega_1}\sum_{i=1}^{2}q_i^sC_i^s, \end{aligned} \tag{4.25a}$$

$$-\left[\nabla_s\cdot\left(\epsilon_r\nabla_s\widetilde{\phi}^s\right)\right]=4\pi\frac{\omega_2}{\omega_1}\sum_{i=1}^{2}q_j^sC_i^s,\quad S_3=\frac{\omega_2}{\omega_1} \tag{4.25}$$

Therefore,

$$\delta_s(\mathbf{r}^s-\mathbf{r}_j^s)=\delta(\mathbf{r}-\mathbf{r}_j)\frac{l^2e_c^2}{\omega_1 k_{\mathrm{B}}T},\ \phi_s^*=\phi^*\frac{e_c}{\omega_1 k_{\mathrm{B}}T},\ \phi_s^0=\phi^0\frac{e_c}{\omega_1 k_{\mathrm{B}}T} \tag{4.26}$$

By (2.2.77), we also have

$$\begin{aligned} \phi_s^*(\mathbf{r}_s) &= \frac{e_c^2}{\omega_1 k_{\mathrm{B}}T}\sum_{j=1}^{N_A}\frac{q_j/e_c}{l\epsilon_m\sqrt{(x_s-x_{s_j})^2+(y_s-y_{s_j})^2+(z_s-z_{s_j})^2}} \\ &= S_1\sum_{j=1}^{N_A}\frac{q_j^s}{\epsilon_m\sqrt{(x_s-x_{s_j})^2+(y_s-y_{s_j})^2+(z_s-z_{s_j})^2}}, \\ S_1 &= \frac{e_c^2}{\omega_1 k_{\mathrm{B}}Tl} \end{aligned} \tag{4.27}$$

$$\begin{aligned} S_1 &= \frac{e_c^2}{\omega_1 k_{\mathrm{B}}Tl} \\ &= \frac{4.8032424\times10^{-10}}{\omega_1\times0.8623\times10^{-4}\times10^{-8}}\left[\frac{\mathrm{esu}^2}{\mathrm{erg}\times\mathrm{cm}}\right] \\ &= \frac{557.0268}{\omega_1}\,[\text{no unit}] \end{aligned} \tag{4.28}$$

Now we consider NP equations

$$\begin{aligned}
\nabla \cdot D(r)\left[\nabla C(r) + \frac{q}{k_{\mathrm{B}}T} C(r)\nabla\widetilde{\phi}(r)\right] &= 0 \\
\frac{1}{l^2}\nabla_s \cdot D(r)\left[\nabla_s C(r) + \frac{\omega_1 k_{\mathrm{B}}T}{e_c}\frac{q}{k_{\mathrm{B}}T} C(r)\nabla_s\widetilde{\phi}^s(r)\right] &= 0 \\
\nabla_s \cdot D^s(r)\left[\nabla_s C(r) + \omega_1 q^s C(r)\nabla_s\widetilde{\phi}^s(r)\right] &= 0 \\
\frac{\omega_2 k_{\mathrm{B}}T}{l^2 e_c^2}\nabla_s \cdot D^s(r)\left[\nabla_s C^s(r) + \omega_1 q^s C^s(r)\nabla_s\widetilde{\phi}^s(r)\right] &= 0, \\
\nabla_s \cdot D^s\left[\nabla_s C^s + \omega_1 q^s C^s \nabla_s\widetilde{\phi}^s\right] &= 0,\ S_2 = \omega_1
\end{aligned} \tag{4.29}$$

The linear PB equation(3.1.7) given by

$$-\nabla\cdot(\epsilon(r)\nabla\phi(r)) + 4\pi k^2\phi(r) = 4\pi\sum_{j=1}^{N_A} q_j\delta(r-r_j),\ r\in\Omega$$

by (4.5) and (4.23), we obtain

$$\begin{aligned}
& -\frac{K_B T\omega_1}{e_c l^2}\nabla_s\cdot(\epsilon_r\nabla_s\phi_s(r_s)) + 4\pi\frac{K_B T}{e_c}\frac{2e_c^2 C^{bulk}}{K_B T}\omega_1\phi_s(r_s) \\
= & -\frac{K_B T\omega_1}{e_c l^2}\nabla_s\cdot(\epsilon_r\nabla_s\phi_s(r_s)) + 8\pi e_c C_s^{bulk}\frac{K_B T}{l^2 e_c^2}\omega_2\omega_1\phi_s(r_s) \\
= & \frac{K_B T\omega_1}{e_c l^2}[-\nabla_s\cdot(\epsilon_r\nabla_s\phi_s(r_s)) + 8\pi C_s^{bulk}\omega_2\phi_s(r_s)]
\end{aligned}$$

Therefore

$$\begin{aligned}
& [-\nabla_s\cdot(\epsilon_r\nabla_s\phi_s(r_s)) + 8\pi C_s^{bulk}\omega_2\phi_s(r_s)] \\
= & \frac{e_c l^2}{K_B T\omega_1} 4\pi\sum_{j=1}^{N_A} q_j\delta(r-r_j) \\
= & 4\pi\sum_{j=1}^{N_A} q_j^s\delta(r_s - r_{s_j})
\end{aligned} \tag{4.30}$$

Scaling nonlinear PB equation (3.1.4)

$$-\nabla\cdot(\epsilon(r)\nabla\phi(r)) + 4\pi k^2\frac{K_B T}{e_c}\sinh(\frac{e_c}{K_B T}\phi(r)) = 4\pi\sum_{j=1}^{N_A} q_j\delta(r-r_j),\ r\in\Omega$$

we have

$$\begin{aligned} & -\nabla\cdot(\epsilon(r)\nabla\phi(r)) + 4\pi k^2\frac{K_BT}{e_c}\sinh(\frac{e_c}{K_BT}\phi(r)) \\ = \quad & \frac{K_BT\omega_1}{e_cl^2}[-\nabla_s\cdot(\epsilon_r\nabla_s\phi_s(r_s)) + 8\pi\frac{\omega_2}{\omega_1}C_s^{bulk}\sinh(\omega_1\phi_s(r_s))] \end{aligned}$$

Therefore

$$[-\nabla_s\cdot(\epsilon_r\nabla_s\phi_s(r_s)) + 8\pi\frac{\omega_2}{\omega_1}C_s^{bulk}\sinh(\omega_1\phi_s(r_s))] = 4\pi\sum_{j=1}^{N_A}q_j^s\delta(r_s - r_{s_j}) \tag{4.31}$$

4.3 Approximation of interface conditions

Due to the interface condition (2.2.86) and ϕ^0 is only defined in $\overline{\Omega}_m$, we remark that the following extrapolation scheme is also described in Section D in [11]. We now derive a nonlinear extrapolation formula for this case from which we can approximate the derivative $\frac{\partial}{\partial x}\phi^0(x_{i+\frac{1}{2}}) = \frac{\partial}{\partial x}\phi^0(x_\gamma)$.

Case I. $\{x_{i-2},\, x_{i-1},\, x_i\} \subset \Omega_m$, $x_{i+\frac{1}{2}} \in \Gamma$, $x_{i+1},\, x_{i+2} \in \Omega_s$ (see Fig. 5.).

$$\begin{aligned} \phi^0(x) &= A_0 + A_1x + A_2x^2 + A_3x^3 + A_4x^4 \\ \frac{\partial}{\partial x}\phi^0(x_\gamma) &\approx A_1 + 2A_2x_\gamma + 3A_3x_\gamma^2 + 4A_4x_\gamma^3 \\ \phi_{i-1} &= A_0 + A_1x_{i-1} + A_2x_{i-1}^2 + A_3x_{i-1}^3 + A_4x_{i-1}^4 \\ \phi_i &= A_0 + A_1x_i + A_2x_i^2 + A_3x_i^3 + A_4x_i^4 \\ \phi_\gamma &= A_0 + A_1x_\gamma + A_2x_\gamma^2 + A_3x_\gamma^3 + A_4x_\gamma^4 \\ \phi_{i+1} &= A_0 + A_1x_{i+1} + A_2x_{i+1}^2 + A_3x_{i+1}^3 + A_4x_{i+1}^4 \\ \phi_{i+2} &= A_0 + A_1x_{i+2} + A_2x_{i+2}^2 + A_3x_{i+2}^3 + A_4x_{i+2}^4 \end{aligned} \tag{4.32}$$

where the values of ϕ_{i+1} and ϕ_{i+2} are obtained by the following two extrapolation formulas similar to (4.32)

$$\begin{aligned} \phi^0(x) &= A_0 + A_1x + A_2x^2 + A_3x^3 \\ \phi_{i-2} &= A_0 + A_1x_{i-2} + A_2x_{i-2}^2 + A_3x_{i-2}^3 \\ \phi_{i-1} &= A_0 + A_1x_{i-1} + A_2x_{i-1}^2 + A_3x_{i-1}^3 \\ \phi_i &= A_0 + A_1x_i + A_2x_i^2 + A_3x_i^3 \\ \phi_\gamma &= A_0 + A_1x_\gamma + A_2x_\gamma^2 + A_3x_\gamma^3 + A_4x_\gamma^4 \\ \phi_{i+1} &= \phi^0(x_{i+1}) \end{aligned} \tag{4.33}$$

$$
\begin{aligned}
\phi^0(x) &= A_0 + A_1 x + A_2 x^2 + A_3 x^3 + A_4 x^4 \\
\phi_{i-2} &= A_0 + A_1 x_{i-2} + A_2 x_{i-2}^2 + A_3 x_{i-2}^3 + A_4 x_{i-2}^4 \\
\phi_{i-1} &= A_0 + A_1 x_{i-1} + A_2 x_{i-1}^2 + A_3 x_{i-1}^3 + A_4 x_{i-1}^4 \\
\phi_i &= A_0 + A_1 x_i + A_2 x_i^2 + A_3 x_i^3 + A_4 x_i^4 \\
\phi_\gamma &= A_0 + A_1 x_\gamma + A_2 x_\gamma^2 + A_3 x_\gamma^3 + A_4 x_\gamma^4 \\
\phi_{i+1} &= A_0 + A_1 x_{i+1} + A_2 x_{i+1}^2 + A_3 x_{i+1}^3 + A_4 x_{i+1}^4 \\
\phi_{i+2} &= \phi^0(x_{i+2})
\end{aligned} \tag{4.34}
$$

Case II. $\{x_{i-\frac{3}{2}}, x_{i+\frac{1}{2}}\} \subset \Gamma$, $\{x_{i-1}, x_i\} \subset \Omega_m$, $x_{i+1} \in \Omega_s$.

$$
\begin{aligned}
\phi^0(x) &= A_0 + A_1 x + A_2 x^2 + A_3 x^3 + A_4 x^4 \\
\frac{\partial}{\partial x}\phi^0(\gamma) &\approx A_1 + 2A_2 x_\gamma + 3A_3 x_\gamma^2 + 4A_4 x_\gamma^3 \\
\phi_{i-1} &= A_0 + A_1 x_{i-1} + A_2 x_{i-1}^2 + A_3 x_{i-1}^3 + A_4 x_{i-1}^4 \\
\phi_i &= A_0 + A_1 x_i + A_2 x_i^2 + A_3 x_i^3 + A_4 x_i^4 \\
\phi_\gamma &= A_0 + A_1 x_\gamma + A_2 x_\gamma^2 + A_3 x_\gamma^3 + A_4 x_\gamma^4 \\
\phi_{i+1} &= A_0 + A_1 x_{i+1} + A_2 x_{i+1}^2 + A_3 x_{i+1}^3 + A_4 x_{i+1}^4 \\
\phi_{i+2} &= A_0 + A_1 x_{i+2} + A_2 x_{i+2}^2 + A_3 x_{i+2}^3 + A_4 x_{i+2}^4
\end{aligned} \tag{4.35}
$$

$$
\begin{aligned}
\phi^0(x) &= A_0 + A_1 x + A_2 x^2 + A_3 x^3 \\
\phi_{\gamma'} &= A_0 + A_1 x_{i-\frac{3}{2}} + A_2 x_{i-\frac{3}{2}}^2 + A_3 x_{i-\frac{3}{2}}^3 \\
\phi_{i-1} &= A_0 + A_1 x_{i-1} + A_2 x_{i-1}^2 + A_3 x_{i-1}^3 \\
\phi_i &= A_0 + A_1 x_i + A_2 x_i^2 + A_3 x_i^3 \\
\phi_\gamma &= A_0 + A_1 x_\gamma + A_2 x_\gamma^2 + A_3 x_\gamma^3 + A_4 x_\gamma^4 \\
\phi_{i+1} &= \phi^0(x_{i+1})
\end{aligned} \tag{4.36}
$$

$$
\begin{aligned}
\phi^0(x) &= A_0 + A_1 x + A_2 x^2 + A_3 x^3 + A_4 x^4 \\
\phi_{\gamma'} &= A_0 + A_1 x_{i-\frac{3}{2}} + A_2 x_{i-\frac{3}{2}}^2 + A_3 x_{i-\frac{3}{2}}^3 \\
\phi_{i-1} &= A_0 + A_1 x_{i-1} + A_2 x_{i-1}^2 + A_3 x_{i-1}^3 + A_4 x_{i-1}^4 \\
\phi_i &= A_0 + A_1 x_i + A_2 x_i^2 + A_3 x_i^3 + A_4 x_i^4 \\
\phi_\gamma &= A_0 + A_1 x_\gamma + A_2 x_\gamma^2 + A_3 x_\gamma^3 + A_4 x_\gamma^4 \\
\phi_{i+1} &= A_0 + A_1 x_{i+1} + A_2 x_{i+1}^2 + A_3 x_{i+1}^3 + A_4 x_{i+1}^4 \\
\phi_{i+2} &= \phi^0(x_{i+2})
\end{aligned} \tag{4.37}
$$

Case III. $\{x_{i-\frac{1}{2}}, x_{i+\frac{1}{2}}\} \in \Gamma$, $x_i \in \Omega_m$, $x_{i+1} \in \Omega_s$

$$\begin{aligned}
\phi^0(x) &= A_0 + A_1 x + A_2 x^2 + A_3 x^3 \\
\frac{\partial}{\partial x}\phi^0(\gamma) &\approx A_1 + 2A_2 x_\gamma + 3A_3 x_\gamma^2 \\
\phi_{\gamma'} &= A_0 + A_1 x_{\gamma'} + A_2 x_{\gamma'}^2 + A_3 x_{\gamma'}^3 \\
\phi_i &= A_0 + A_1 x_i + A_2 x_i^2 + A_3 x_i^3 \\
\phi_\gamma &= A_0 + A_1 x_\gamma + A_2 x_\gamma^2 + A_3 x_\gamma^3 \\
\phi_{i+1} &= A_0 + A_1 x_{i+1} + A_2 x_{i+1}^2 + A_3 x_{i+1}^3
\end{aligned} \tag{4.38}$$

$$\begin{aligned}
\phi^0(x) &= A_0 + A_1 x + A_2 x^2 \\
\phi_{\gamma'} &= A_0 + A_1 x_{\gamma'} + A_2 x_{\gamma'}^2 \\
\phi_i &= A_0 + A_1 x_i + A_2 x_i^2 \\
\phi_\gamma &= A_0 + A_1 x_\gamma + A_2 x_\gamma^2 \\
\phi_{i+1} &= \phi^0(x_{i+1})
\end{aligned} \tag{4.39}$$

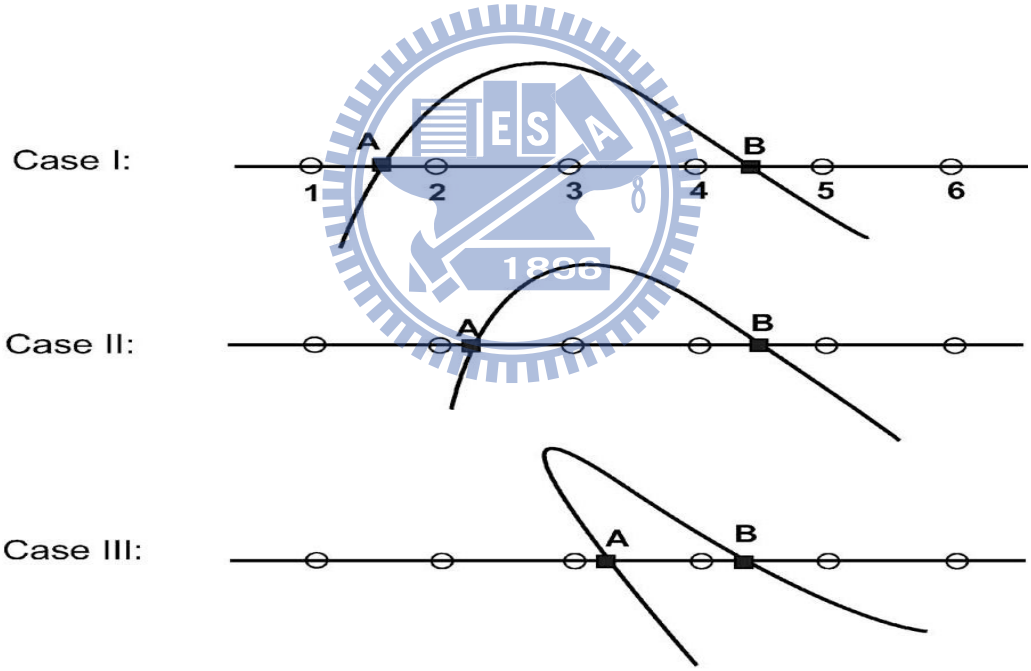

Figure. 5. The schematic diagram[11] for three different case

we given the notation transformation by following

Notation (Fig. 5.):	1	2	3	4	5	6
Notation in extrapolation formula:	x_{i-3}	x_{i-2}	x_{i-1}	x_i	x_{i+1}	x_{i+2}

and the interface points A, B are denoted

	Case 1	Case 2	Case 3
A:	$x_{i-\frac{5}{2}}$	$x_{i-\frac{3}{2}}$	$x_{i-\frac{1}{2}}$
B:	$x_{i+\frac{1}{2}}$	$x_{i+\frac{1}{2}}$	$x_{i+\frac{1}{2}}$

4.4 Numerical results for test cases

All results of test cases are given in this section where the second-order convergence has been obtained. Now we consider test csae in section 2.3.

Example 4.2 Consider real GA channel structure and dielectric constant $\epsilon_m = 1$, $\epsilon_s = 80$. Jump condition are given by $[\phi] = 0$ and $[\epsilon\phi_{\mathbf{n}}] = g \neq 0$ (2.3.12). Numerical results for the Poisson problem are shown in Table 4.4.1 with good $O(h^2)$ convergence. Numerical results of the same exact solution (2.3.1) used in [24] for the GA channel are also presented for comparison. Note that the MIB method of Wei et al. [24] requires more than 27 FD grid points whereas ours requires only 7 under the assumption (2.2.4). The method with (2.2.52), (2.2.55), and (2.2.70) in the primitive form (sec. 2.2.3) gave perfect results as shown in following table for linear PNP problems.

Table 4.4.1. Linear, Ours vs Wei's [24] MIB				
	Ours test		Wei's [24] test	
h in Å	E_∞	Order	E_∞	Order
2	0.4466			
1	0.0922	2.28	0.1400	
0.5	0.0228	2.02	0.0271	2.36
0.25	0.0057	2.00	0.0152	0.84

Table 4.4.1 : Comparison of convergence order between Wei's test and ours test

Table 4.4.2. Linear								
	Dirichlet BC				Robin BC			
mesh sise	P	NP1	NP2	Time	P	NP1	NP2	Time
2	0.4466	1.0203	1.1903		0.4466	1.0302	1.4471	
1	0.0922	0.0457	0.0360		0.0922	0.0451	0.0434	
0.5	0.0228	0.0103	0.0072	1m14s	0.0228	0.0103	0.0081	1m14s
0.25	0.0057	0.0025	0.0017	10m28s	0.0057	0.0025	0.0018	10m31s

Table 4.4.2 : Use of different boundary conditions at the interface

Example 4.3. For nonlinear case, consider real GA channel structure and dielectric

constant $\epsilon_m = 1$, $\epsilon_s = 80$. Jump condition are given by $[\phi] = 0$ and $[\epsilon\phi_{\mathbf{n}}] = g \neq 0$ (2.3.12).

Table 4.4.3. Nonlinear												
	Wei's [24]						Ours					
h Å	P	Ord	NP1	Ord	NP2	Ord	P	Ord	NP1	Ord	NP2	Ord
1	0.1400		0.0841		0.0554		0.0925		0.0327		0.0168	
0.5	0.0272	2.36	0.0167	2.33	0.0123	2.17	0.0228	2.02	0.0074	2.14	0.0037	2.18
0.25	0.0152	0.84	0.0046	1.84	0.0039	1.65	0.0057	2.00	0.0018	2.04	0.0009	2.04

Example 4.4. Consider nonlinear case, real GA channel structure and dielectric constant $\epsilon_m = 1$, $\epsilon_s = 80$. Jump condition are given by $[\phi] = 0$ and $[\epsilon\phi_{\mathbf{n}}] = g \neq 0$ (2.3.12). But add diffusion function (4.19) in NP equation

Table 4.5.(n=2)						
h Å	P	Ord	NP1	Ord	NP2	Ord
1	0.0924		0.0344		0.0194	
0.5	0.0228	2.02	0.0076	2.18	0.0038	2.35
0.25	0.0057	2.00	0.0019	2.00	0.0009	2.08

The following two tests is to consider different parameters (ω_1, ω_2) for nonlinear Poisson-Boltzmann (PB) equation (3.1.4). The parameters (ω_1, ω_2) only be applied at the boundary (4.12a) (4.12b) and $C_i^{bulk} = 0.1$ molar, $V_0 = 0$ (4.1).

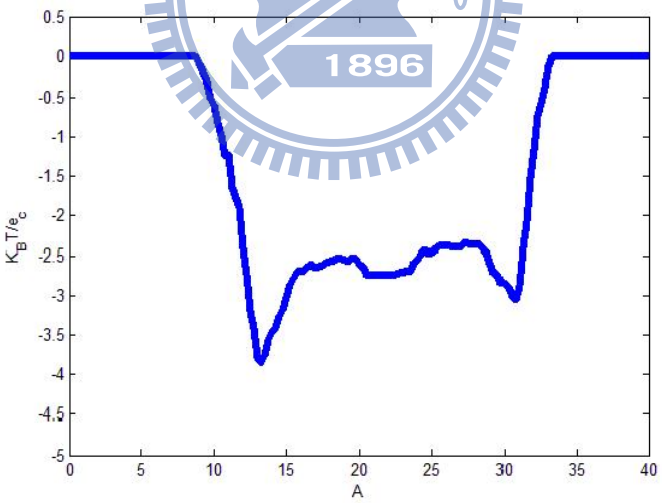

Figure. 6. (ω_1, ω_2)=(300,100)

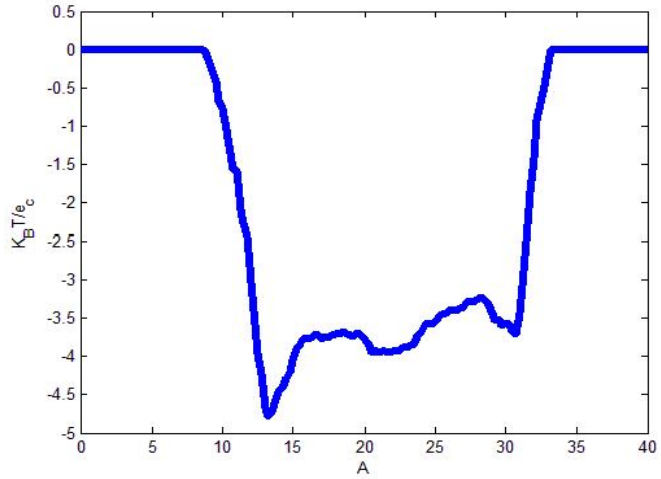

Figure. 7. (ω_1, ω_2)=(300,150)

5 Conslusions

By the test case in section 2.3, we get a better results than [24] (in Table 3.1). However, the parameters ω_1 and ω_2 in (4.23) are very sensitive to real PNP and PB models from which we are still unable to obtain good results that are comparable to those in [24]. In the future, we have to go to explore the relationship between mathematical parameters (ω_1, ω_2) and physical effects and give a reasonable explanation. If we obtain good results for PNP equation, the I-V curve predicted by the model and we can compare between the PNP prediction and experimental data. The accuracy of the PNP model can thus be determined to simulate the ion channels.

In general, the PNP equations can be added to the time parameters and become 4D problem, i.e., $-\nabla_r \cdot J_i(r,t) = \partial C_i(r,t)/\partial t$. Moreover, we may also consider the influence of temperature as a function $T(r,t)$ is the the absolute temperature depends on the location r and time t.

Moreover, quantum effects will be taken into account, i.e., we will consider a quantum corrected Poisson-Nernst-Planck model [17]. In such a small ion channel, it is very reasonable to consider the quantum effects and it may lead to simulation results that are closer to the experimental data.

References

[1] A. Aksimentiev, M. Sotomayor, and D. Wells, Membrane proteins tutorial, Theoretical and Computational Biophysics Group, University of Illinois at Urbana-Champaign (2009).

[2] V. Barcilon, Ion flow through narrow membran channels: part I. SIAM J. APPL. MATH, 52(5):1391– 1404, 1992.

[3] V. Barcilon, D. Chen, and R. Eisenberg, Ion flow through narrow membrane channels: Part ii. SIAM J. Appl. Math, 52:1405–1425, October 1992.

[4] S.-H. Chung and S. Kuyucak, Recent advances in ion channel research. Biochimica et Biophysica Acta, 1565:267–286, 2002.

[5] I-L. Chern, J.-G. Liu, and W.-C. Wang, Accurate evaluation of electrostatics for macromolecules in solution, Methods Appl. Anal. 10 (2003) 309—328.

[6] C. de Falco, J. W. Jerome, and R. Sacco, A self-consitent iterative scheme for the one-dimensional steady-state transistor calculations. IEEE Trans. Ele. Dev., 11:455–465, 1964.

[7] D. Chen, and G.-W. Wei, Quantum dynamicsin continuum for ion channel transport, preprint (2010).

[8] D. P. Chen, V. Barcilon, and R. S. Eisenberg, Constant fields and constant gradients in open ionic channels, Biophys. J. 61 (1992) 1372—1393.

[9] R. S. Eisenberg, Multiple scales in the simulation of ion channels and proteins, J. Phys. Chem. C 114 (2010) 20719—20733.

[10] B. Eisenberg and W. S. Liu, Poisson-Nernst-Planck systems for ion channels with permanent charges. SIAM J. Math, Analy, 38(6):1932–1966, 2006.

[11] W. Geng, S. Yu, and G. Weia, Treatment of charge singularities in implicit solvent models, J. Chem. Phys. 127 (2007) 114106.

[12] B. Hille, Ionic Channels of Excitable Membranes, 3rd Ed., Sinauer Associates Inc., Sunderland, MA, 2001.

[13] M. Hacker, W. Messer, and K. Bachmann. Pharmacology: Principles and Practice. Academic Press, 2009.

[14] M. Hacker, W. Messer, and K. Bachmann. Pharmacology: Principles and Practice. Academic Press, 2009.

[15] W. Humphrey, A. Dalke, and K. Schulten, VMD - Visual Molecular Dynamics, J. Molec. Graphics, 14 (1996) 33-38.

[16] Y. W. Jung, B. Z. Lu, and M. Mascagni, A computational study of ion conductance in the kcsa k+ channel using a Nernst-Planck model with explicit resident ions. J. Chem. Phys., 131(215101), 2009.

[17] J.-L. Liu, Lecture Notes on Poisson-Nernst-Planck Modeling and Simulation of Biological Ion Channels, 2012.

[18] B. Lu and J. A. McCammon, Molecular surface-free continuum model for electrodiffusion processes, Chem. Phys. Lett. 451 (2008) 282—286.

[19] D. Marx and J. Hutter, Ab initio molecular dynamics: Theory and implementation. Modern Methods and Algorithms of Quantum Chemistry, J. Grotendorst (Ed.), John von Neumann Institute for Computing, Julich, NIC Series, 3:329–477, 2000.

[20] Popular Information, Nobelprize.org. 18 Jan 2011, http://nobelprize.org/ nobel_prizes/chemistry/laureates/2003/public.html.

[21] D. Purves, G. J. Augustine, D. Fitzpatrick, L. C. Katz, A. S. LaMantia, J. O. McNamara, and S. M. Williams. Neuroscience, 2nd edition. Sunderland, MA: Sinauer Associates, 2001.

[22] J. W. Slotboom, Computer-aided two-dimensional analysis of bipolar transistors, IEEE Trans. Elec. Dev. ED-20 (1973) 669-679.

[23] N. A. Simakov and M. G. Kurnikova, Soft wall ion channel in continuum representation with application to modeling ion currents in -Hemolysin, J. Phys. Chem. B 114 (2010) 15180—15190.

[24] Q. Zheng, D. Chen, and G.-W. Wei, Second-order Poisson Nernst-Planck solver for ion channel transport, J. Comp. Phys. 230 (2011) 5239-5262.